I. A. Kondurov, A. M. Nikitin, A. I. Yegorov, and Yu. K. Zalite, Phys. Letters 30B, 332 (1969).
[14]M. Cambiagni, F. Fossati, and T. Pinelli, Nuovo Cimento 59B, 236 (1969).
[15]T. Krogulski, J. Chwaszczewska, M. Dakowski, E. Piasecki, M. Sowinski, and J. Tys, Nucl. Phys. A128, 219 (1969).
[16]Z. I. Soloveva, Yadern. Fiz. 8, 454 (1969) [transl.: Soviet J. Nucl. Phys. 8, 264 (1969)].
[17]T. D. Thomas and S. L. Whetstone, Phys. Rev. 144, 1060 (1966).
[18]R. A. Atneosen, T. D. Thomas, and G. T. Garvey, Phys. Rev. 139, B307 (1965).
[19]E. Piasecki, M. Dakowski, T. Krogulski, J. Tys, and J. Chwaszczewska, Phys. Letters 33B, 568 (1970).
[20]N. A. Perfilov and Z. I. Solov'eva, Zh. Eksperim. i Teor. Fiz. 37, 1157 (1959) [transl.: Soviet Phys.-JETP 10, 824 (1960)].
[21]R. Ramanna, K. G. Nair, and S. S. Kapoor, Phys. Rev. 129, 1350 (1963).
[22]V. A. Hattangadi, T. Methasiri, D. M. Nadkarni, R. Ramanna, and P. N. Rama Rao, in *Proceedings of the Symposium on the Physics and Chemistry of Fission, Salzburg, 1965* (International Atomic Energy Agency, Vienna, Austria, 1965), Vol. II, p. 397.
[23]I. Halpern, in *Proceedings of the Symposium on the Physics and Chemistry of Fission, Salzburg, 1965* (see Ref. 22), Vol. II, p. 369.
[24]N. Feather, in *Proceedings of the Symposium on the Physics and Chemistry of Fission, Salzburg, 1965* (see Ref. 22), Vol. II, p. 387.
[25]N. Feather, Phys. Rev. 170, 1127 (1968).
[26]N. Feather, in *Proceedings of the Second International Atomic Energy Symposium on Physics and Chemistry of Fission, Vienna, Austria, 1969,* (International Atomic Energy Agency, Vienna, Austria, 1969), p. 83.
[27]P. Vitta, Nucl. Phys. A170, 417 (1971).
[28]A. Katase, J. Phys. Soc. Japan, 25, 933 (1968).

PHYSICAL REVIEW C VOLUME 5, NUMBER 6 JUNE 1972

Level Scheme of ^{235}U and the Distribution of Single-Particle Strength in Its Excited States*

Frank A. Rickey
Los Alamos Scientific Laboratory, University of California, Los Alamos, New Mexico 87544, and Physics Department, Purdue University, Lafayette, Indiana 47907

and

E. T. Jurney and H. C. Britt
Los Alamos Scientific Laboratory, University of California, Los Alamos, New Mexico 87544
(Received 7 February 1972)

The spectra of low-lying states of ^{235}U have been studied using the reactions ^{233}U$(t,p)^{235}$U, ^{235}U$(d,d')^{235}$U, ^{234}U$(d,p)^{235}$U, ^{236}U$(d,t)^{235}$U, and ^{234}U$(n,\gamma)^{235}$U. Using intensity ratios and angular distributions from the charged-particle reactions, primary γ-ray excitations, patterns of γ-ray deexcitations, and rotational-band systematics, 80% of the levels observed up to 1500 keV have been assigned to 23 individual rotational bands. Some of the rotational bands can be associated with expected single-particle excitations, but in many cases it is shown that the single-particle strength is fragmented, giving rise to several rotational bands with similar properties. Mechanisms for this fragmentation are discussed and the distribution of single-particle strength over the states observed is examined and compared with theoretical predictions. The neutron binding energy for ^{235}U is determined to be 5297.6±0.5 keV.

I. INTRODUCTION

In recent years level spectra of deformed nuclei in the rare-earth region have been extensively investigated,[1] and the Nilsson model[2] of single-particle excitations has been found to describe very well the low-energy structure of odd-A nuclei in this region. However, at excitation energies above about 1 MeV the Nilsson description must be modified to include collective three-quasiparticle excitations,[3,4] corresponding to the coupling of a Nilsson single-particle state to a one-phonon vibrational excitation of the core (a particle+phonon state). In the rare-earth region the lowest one-phonon states are usually of the quadrupole type, occurring typically around 1 MeV.

In the actinide region one-phonon core excitations of the octupole type also lie low in excitation energy, and are expected to make the structure of odd-A actinide nuclei complex at low excitation energies. There are, for example, six known vibrational states in ^{234}U below 1.5 MeV, the lowest being a $K^{\pi}=0^{-}$ octupole state at 788 keV.[5,6] Braid, Chasman, Erskine, and Fried-

man[7] (referred to hereafter as the Argonne group) have reported results in the study of ^{235}U using the reactions ^{234}U$(d, p)^{235}$U and ^{236}U$(d, t)^{235}$U, and their work demonstrates the complexity of the level spectrum.

Much of the progress in the study of deformed odd-A nuclei has been due to the use of charged-particle nuclear reactions. These reactions have advantages in certain respects over the study of states by γ-ray spectroscopy. Charged-particle reactions populate excited states directly, so that the major uncertainty in level positions is related to the experimental energy resolution. Higher angular momentum transfers can be observed than in (n, γ) experiments so that states with a wide range of spin and parity can be populated in any given reaction. Finally the particular reaction can be selected to populate specific components of the states; for example, a (d, p) reaction populates only single-particle components. On the other hand the energy resolution is generally poorer in a charged-particle experiment than it is in γ spectroscopy. The combination of the two techniques can be useful in the study of nuclear structure.

The present work is an attempt to study the character of states of ^{235}U by the use of several complementary reactions. Targets are available to populate ^{235}U levels by the (d, p), (d, t), (t, p), (d, d'), and (n, γ) reactions. The (d, p) and (d, t) reactions are expected to populate, respectively, single-particle and single-hole components of the states. Both of these reactions have been studied by the Argonne group[7] at an incident deuteron energy of 11.97 MeV, which is below the Coulomb barrier. In the present work the incident deuteron energy was 20 MeV, well above the Coulomb barrier. The cross sections for higher l transfers are enhanced, and the spectrum of states populated is more complete than in the previous Argonne data. The (t, p) and (d, d') reactions are shown to preferentially populate states based on the ground states of ^{233}U and ^{235}U, respectively. The (n, γ) reaction yields two distinct types of information; the high-energy transitions from the $\frac{1}{2}^+$ capture state directly populate low-spin states, while the low-energy transitions fill out the details of the decay scheme.

TABLE I. Uranium target isotopic compositions for the charged-particle reaction experiments.

Target	233	234	235	236	238
233	0.9796	0.0137	0.0007		0.006
234		0.997	0.003		
235		0.0103	0.9325	0.0028	0.0544
236			0.001	0.998	0.000 05

For a limited number of states, angular distributions for the reaction ^{234}U$(d, p)^{235}$U provide information on the l transfers involved in the population of particular states. Additional information from the (n, γ) data and rotational energy systematics help to provide spin, parity, and excitation energy information on most of the states in the spectrum up to an energy of ~1500 keV.

The primary goal of this work is to assign the observed energy levels to various rotational bands using the available experimental information and to examine the way in which the large number of low-lying core excitations affect predictions of the Nilsson model. These effects will be discussed in the framework of existing theories of particle +phonon admixtures in the excited states of deformed odd-A nuclei.

II. EXPERIMENTAL METHOD AND DATA

A. Charged-Particle Data

The deuteron and triton beams used for the charged-particle experiments were obtained from the Los Alamos Scientific Laboratory three-stage electrostatic accelerator. The beam energy was 20 MeV in all instances, and the beam current varied between 0.5 and 1.0 μA.

Targets used in the experiment were uranium oxide vacuum-evaporated onto 50–80-μg/cm^2 carbon backings. The target thicknesses varied from 100–200 μg/cm^2 for the ^{234}U and ^{236}U targets to 800–1000 μg/cm^2 for the ^{233}U and ^{235}U targets. Isotopic compositions of the targets are given in Table I.

The reaction products were analyzed in a magnetic spectrograph based on the design of Elbek,[8] using photographic plates on the focal curve as detectors. The plates were manually scanned and the number of tracks per 0.15-mm strip along a plate was recorded. The beam current was integrated for each exposure by measuring the charge collected by a Faraday cup, with electron emission suppressed magnetically. An elastic scattering measurement was taken before each exposure, and using previous measurements of the elastic cross section (see Appendix), the product of the target thickness and the solid angle of the spectrograph was determined. The variation of the solid angle along the focal curve was used along with these two quantities to reduce the data to cross sections. Errors in the cross sections can be grouped into two kinds, random and systematic. Systematic errors arise from the measurement of the elastic cross section (see Appendix), the measurement of integrated charge for

the short elastic exposures, and the acceptance criteria used in the plate scanning. These errors are estimated to produce a total systematic error of less than 10%. Other counting errors are assumed to be random, and are of the order of 2%. The largest random error arises from the small number of tracks obtained for many groups.

Because of the close spacing of particle groups in the data, the location and magnitude of each group was determined by a least-squares-fitting procedure, assuming each particle group to have a distribution in energy of a skewed Gaussian with exponential tail. The energy of each group was then determined from a calibration based on the 5.3042-MeV α group from a ^{210}Po source.

Data were obtained for four different reactions populating states in ^{235}U: ^{234}U$(d, p)^{235}$U, at 15, 20, 30, 35, 40, 45, 55, 70, and 105°; ^{236}U$(d, t)^{235}$U, at 20, 30, 40, 50, 60, and 70°; ^{233}U$(t, p)^{235}$U at 12, 20, and 30°; and ^{235}U$(d, d')^{235}$U at 60 and 90°. The energy resolution for the (d, p) and (d, t) data varied between 10 and 15 keV, while for the (t, p) and (d, d') data it was approximately 20 keV, owing to the thicker targets. Typical spectra for the four reactions are shown in Fig. 1. Although the errors in excitation energies obtained from these data should be random errors of the order of 2–3 keV, for energy resolutions of 10–15 keV, systematic errors as large as 10 keV were found in a comparison with known levels. We believe that the contraction or expansion of the emulsions during slightly different developing procedures is the major cause of this error. In order to correct for the distortion of the energy scale two groups in each spectrum were forced to have the correct excitation energies as determined in the

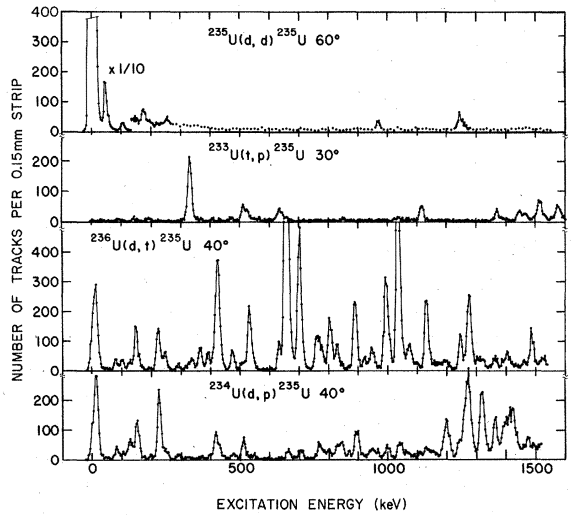

FIG. 1. Typical spectra for the charged-particle reactions leading to states in ^{235}U.

^{234}U(n, γ) reaction. Nearly all the systematic error has thus been removed, and the remaining deviations are found to be in the range ±2 keV.

Values of the l transfer were determined for some of the states by comparison of the ^{234}U(d, p)-^{235}U angular distributions with calculations from the distorted-wave Born-approximation (DWBA) code JULIE.[9] A few of the comparisons are shown in Fig. 2. The extraction of l transfer is complicated by the fact that many of the peaks seen in Fig. 1 are complex and the cross section determination is uncertain, even though a least-squares procedure was used. A more complete discussion of the reliability of the process can be found in the Appendix.

A summary of the energy levels populated in the various reactions along with suggested l transfers is presented in Table II. The errors quoted are a combination of the 2-keV estimated systematic errors and the statistical errors.

B. (n, γ) Experiments

The γ-ray spectrum following thermal-neutron capture in ^{234}U was obtained with the internal target facility at the Los Alamos Omega West Reactor; a detailed description of this facility has been published.[10] In all the measurements to be described in this section, use was made of an 18-mg target of UO_2 containing 99.7% ^{234}U and 0.3% ^{235}U. From the thermal-neutron cross-section values,[11] $\sigma_c \approx \sigma_a = 95 \pm 7$ b for ^{234}U and $\sigma_F = 577.1 \pm 0.9$ b for ^{235}U, the ratio of fissions to ^{234}U captures in the target is found to be 0.018.

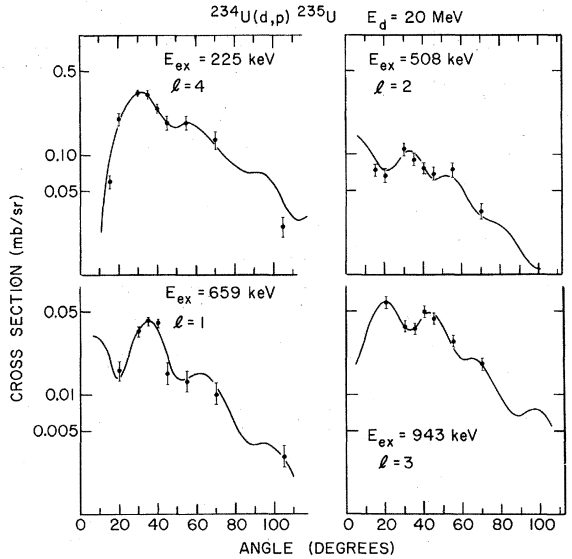

FIG. 2. Comparison of experimental angular distributions with DWBA calculations for selected states populated in the reaction ^{234}U$(d, p)^{235}$U.

TABLE II. Levels observed in the charged-particle reactions. Energies in keV are relative to ground state. Cross sections (mb/sr) for a single angle are included. Parentheses indicate less certainty in l-value assignment.

$E(d,p)$	ΔE	$\frac{d\sigma}{d\omega}(40°)$	$E(d,t)$	ΔE	$\frac{d\sigma}{d\omega}(40°)$	$E(t,p)$	ΔE	$E(d,d')$	ΔE	l
0 [a]	2.1	0.128	0 [a]	2.1	0.214			0 [a]		
13	2.4	0.319	13	2.2	0.379					
								47	1.8	
52	2.6	0.007	52	2.1						
83	2.6	0.047	83	3.4	0.044					(4)
103	2.6	0.023	103	3.2	0.028			105	2.2	
131	2.2	0.063	129	2.2	0.047					2
151	3.2	0.136	151	2.4	0.184					
171	3.9	0.004	166	2.2	0.028			174	3.1	
197	2.4	0.014	197	3.0	0.004					
225	b	0.230	225	b	0.216					4
247	2.1	0.029	247	2.0	0.093					
259	2.1	0.013	257	2.0	0.008			257	4.0	
293	2.2	0.020	293	3.2	0.017					
			324	4.1	0.011					
329	3.9	0.010	335	3.6	0.051	331	3.1			
368	5.7	0.010	366	3.9	0.103					
395	2.6	0.017	393	2.6	0.054					
415	2.2	0.091	413	2.0	0.133					
427	2.5	0.043	426	2.0	0.537					
			437	2.1	0.024					
475	3.4	0.021	474	2.7	0.080					
494	3.2	0.004								
511	2.8	0.077	509	3.4	0.023	511	4.0			2
532	2.9	0.027	532	2.0	0.279					
			540	3.0	0.034					
548	2.2	0.006	550	2.4	0.004					
585	3.2	0.125	587	4.3	0.003					
590	2.2	0.003								
604	4.2	0.001	606	2.2	0.001					
639	2.0	0.143	635	3.0	0.117	636	3.0			
661	3.1	0.034	658	2.8	1.814					1
			675	2.4	0.051					
			692	2.1	0.010					
703	2.5	0.032	702	2.2	0.693					
711	2.4	0.002								
729	2.9	0.004	725	2.1	0.010					
763	3.0	0.052	761	3.4	0.137					
771	3.1	0.035								
			777	4.1	0.074					
794	3.1	0.024	797	2.0						
804	2.9	0.031	804	2.0	0.249					
			821	2.0	0.012					
827	2.4	0.050	828	2.0	0.091					
844	3.3	0.059	844	2.1						
869	2.9	0.016								
882	2.0	0.027								
			887	2.5	0.345					
893	2.0	0.063								
913	2.1	0.023								
924	4.6	0.009	921	2.2	0.032					
942	2.1	0.034	945	2.2	0.055					3
961	2.7	0.019								

TABLE II *(Continued)*

$E(d,p)$	ΔE	$\frac{d\sigma}{d\omega}(40°)$	$E(d,t)$	ΔE	$\frac{d\sigma}{d\omega}(40°)$	$E(t,p)$	ΔE	$E(d,d')$	ΔE	l
970	4.1	0.003	967	2.2	0.002			969	4.2	
983	2.1	0.008								
991	3.4	0.040	993	2.4	0.505					
1002	2.2	0.046	1000	3.9	0.269					
1030	2.4	0.005								
1038	2.1	0.040	1035	b	1.16					
1049	2.1	0.029	1052	2.3						
1057	2.2	0.011								
1072	5.4	0.014	1073	2.1	0.128					
			1095	2.8	0.038					
1103	2.1	0.012								
1112	2.5	0.010				1115	3.2			
1130	3.3	0.030	1129	2.1	0.335					
1135	2.3	0.035								
1150	2.6	0.015	1149	2.4	0.017					
1178	2.0	0.024								
			1186	2.4	0.009					
1192	2.4	0.093	1194	2.4	0.012					1
1203	2.3	0.072								1
1212	2.1	0.064								
1233	2.8	0.056								
1242	2.3	0.042	1243	3.0	0.131			1242	3.1	
1258	2.2	0.137								
			1266	2.0						
1273	b	0.248	1274	2.0	0.394					
1287	2.6	0.072								
1297	2.5	0.105								(2)
			1303	2.3	0.014					
1314	2.3	0.182	1314	2.4	0.024					
1321	2.4	0.103	1323	2.7	0.044					
1342	2.1	0.019	1341	2.2	0.009					
1352	2.4	0.029	1355	2.6	0.022					
1364	2.0	0.125	1363	3.0	0.025					
1372	2.1	0.101								
1385	2.5	0.047	1385	2.2	0.015					
1395	2.2	0.088								(1)
1403	2.1	0.197	1400	2.5	0.052					
1411	2.0	0.039	1413	2.9	0.005					
1422	2.1	0.121								
1435	2.1	0.032	1429	2.3	0.003					
1442	2.9	0.034	1439	2.8						
1455	2.9	0.034	1458	3.2	0.019					
1474	2.7	0.034								
1482	2.0	0.038	1485	2.2	0.106					
1495	5.1	0.013	1494	2.8	0.018					
1511	3.4	0.021								
1524	2.3	0.030	1521	2.1	0.018					
1528	2.0	0.030	1528	2.3	0.015					
1543	2.1	0.027	1539	2.6	0.004					
1559	3.5	0.013								

[a] Even though measured energies are the same, the (d,p) and (d,t) reactions populate the $\frac{1}{2}^+$ state, while the (d,d') reaction populates the $\frac{7}{2}^-$ state.

[b] These levels are the additional calibration points for the different spectra.

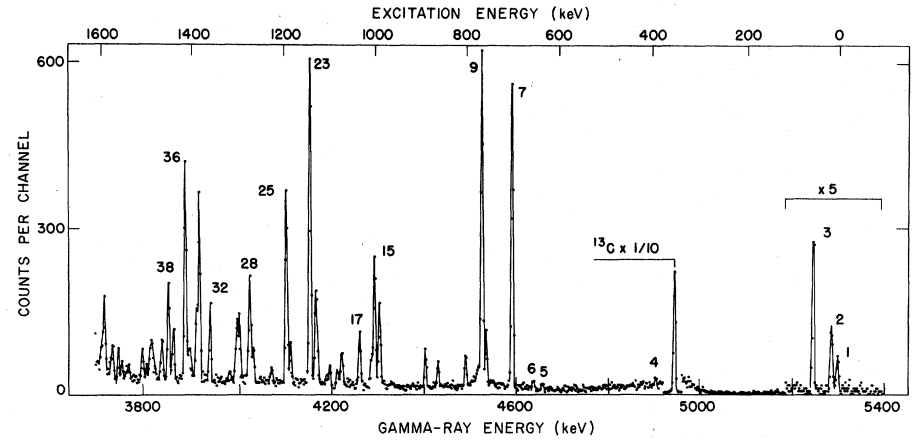

FIG. 3. Spectrum of high-energy γ rays from the reaction ^{234}U$(n, \gamma)^{235}$U. The strong ^{13}C peak is from neutron capture in the graphite target holder.

Three experimental arrangements were used to measure three separate energy intervals of the spectrum. The high-energy portion of the spectrum (3500 to 5300 keV, Fig. 3) was obtained with a 6-cm^3 Ge(Li) detector placed inside a large optically divided NaI annulus. By requiring the pulses from the central Ge(Li) detector to be in coincidence with pulses from each half of the annulus corresponding to the annihilation quantum energy, the background is reduced substantially and only double-escape peaks appear in the spectrum. Energies and intensities of the unknown high-energy γ rays were determined with respect to transitions having well-known energies and partial capture cross sections in the capture γ-ray spectrum of ^{15}N. This calibration spectrum was produced with a small weighed sample of melamine.

In the 250–1500-keV energy region (Fig. 4) the annulus was operated in anticoincidence with a 26-cm^3 Ge(Li) detector to reduce that part of the background originating from escaping Compton scattered quanta. The lowest energy portion of the spectrum, 12 to 250 keV, was obtained with

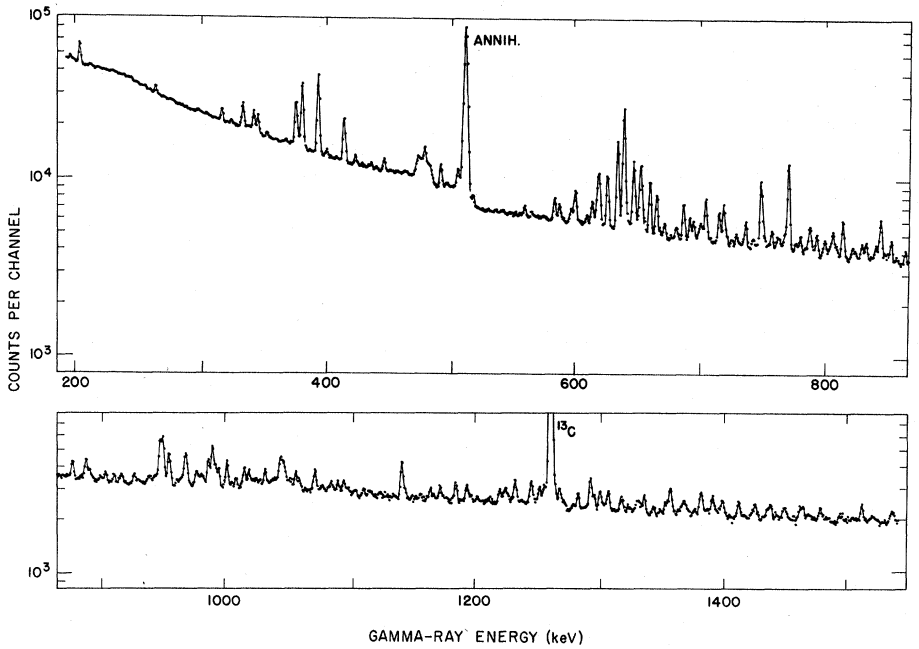

FIG. 4. Spectrum of low-energy γ rays from the reaction ^{234}U$(n, \gamma)^{235}$U. The strong ^{13}C peak at 1261.75 keV is from capture in the graphite target holder; the broad peak at ~480 keV is from ^{10}B$(n, \alpha)^7$Li due to a small amount of boron impurity in the holder.

a small, high-resolution Ge(Li) detector, with no surrounding annulus, placed in the external γ-ray beam. Energy calibration of both the low-energy segments was done with a series of radioactive standards. Intensities in millibarns of partial capture cross section were determined relative to the capture cross section of Au leading to the well-known 411-keV transition in ^{198}Hg.

Thermal-neutron capture by the even-even nucleus ^{234}U leads to a $\frac{1}{2}^+$ compound state in ^{235}U which will generally deexcite by electric or magnetic dipole radiation to lower states with $J^\pi = \frac{1}{2}^\pm$ or $\frac{3}{2}^\pm$. Thus the stronger transitions in the high-energy capture γ-ray spectrum shown in Fig. 3 correspond to the excitation of such low-lying levels in ^{235}U. The transitions observed in the high- and low-energy regions are given in Tables III and IV, respectively.

Through the identification of γ-ray cascades involving strong transitions the neutron binding energy for ^{235}U was determined to be 5297.6 ± 0.5 keV.

III. ASSIGNMENTS

The same basic method for assigning levels to rotational bands was used for all of the data. The underlying assumption for all assignments is that the excitation energies of members of the same rotational band are given by[12]

$$E_j = E_j^0 + \frac{\hbar^2}{2I}[\,j(j+1) - 2K^2 + \delta_{K,1/2} a(-1)^{j+1/2}(j+1/2)\,].$$

The higher-order terms in $[\,j(j+1)]^n$ have been neglected because their effect is small for the angular momenta involved here. The expression contains only the diagonal Coriolis terms, however, and the off-diagonal terms may have significant effects on the energy spacings in cases where two bands with K differing by 1 lie close toegther in energy. Another difficulty is the experimental errors of the excitation energies, which are about ±2 keV for the charged-particle data. This would not be a severe problem if the level density were low, but as the level density increases, the probability increases of uncorrelated sets of levels agreeing with the calculated rotational spacings within the errors involved. Additional information is clearly needed. In the present work this additional information comes from several sources. In some cases l values have been extracted from the ^{234}U(d, p) angular distributions, and these l values must support the assumed spin and parity of the state in question. The high-energy (n, γ) transitions are also important. The high-energy transitions originate from a $\frac{1}{2}^+$ capture state, and, if dipole radiation is assumed to be the dominant deexcitation mech-

TABLE III. High-energy γ rays from ^{234}U$(n, \gamma)^{235}$U corresponding to excitations up to 1.5 MeV in ^{235}U.

Number	E_γ (keV)	E_{exc} (keV)	dE_{ex} (keV)	I_γ ($\gamma/10^3 n$)	dI_γ ($\gamma/10^3 n$)	Number	E_γ (keV)	E_{exc} (keV)	dE_{ex} (keV)	I_γ ($\gamma/10^3 n$)	dI_γ ($\gamma/10^3 n$)
1	5297.9	−0.3	0.6	0.18	0.06	21	4191.6	1106.0	1.1	0.18	0.10
2	5284.6	13.0	0.5	0.33	0.09	22	4168.0	1129.6	0.3	3.7	0.7
3	5245.9	51.6	0.3	0.78	0.18	23	4155.1	1142.5	0.3	9.5	2.0
4	4904.4	393.1	1.0	0.20	0.10	24	4112.2	1185.4	0.4	0.90	0.20
5	4658.2	639.4	1.0	0.18	0.06	25	4103.4	1194.2	0.3	5.8	1.2
6	4639.1	658.5	0.8	0.27	0.08	26	4071.0	1226.6	0.6	0.46	0.13
7	4593.9	703.7	0.3	7.7	1.6	27	4031.9	1265.7	0.6	1.1	0.3
8	4536.8	760.8	0.3	1.1	0.3	28	4024.7	1272.9	0.4	3.1	0.7
9	4527.8	769.8	0.3	8.9	1.8	29	4000.5	1297.1	0.4	1.6	0.4
10	4519.3	777.7	1.0	0.37	0.12	30	3995.4	1302.2	0.5	1.6	0.4
11	4492.3	805.3	0.3	0.90	0.20	31	3981.2	1316.4	1.3	0.19	0.11
12	4432.6	865.0	0.3	0.68	0.16	32	3939.0	1358.6	0.3	2.1	0.5
13	4405.6	892.0	0.3	1.0	0.2	33	3915.1	1382.5	0.3	5.5	1.1
14	4305.2	992.4	0.3	0.21	0.05	34	3909.1	1388.5	0.4	2.1	0.5
15	4295.0	1002.6	0.3	3.7	0.8	35	3893.1	1404.5	0.5	1.0	0.3
16	4288.8	1008.8	1.0	1.0	0.4	36	3884.7	1412.9	0.3	6.4	1.3
17	4262.4	1035.2	0.3	1.5	0.4	37	3858.2	1439.4	0.5	1.1	0.3
18	4223.9	1073.7	0.5	1.0	0.2	38	3848.6	1449.0	0.3	3.1	0.7
19	4214.7	1082.9	0.7	0.33	0.10	39	3834.8	1462.8	0.4	1.2	0.3
20	4197.9	1099.7	0.5	0.46	0.13	40	3813.7	1483.9	0.9	0.93	0.25
						41	3809.5	1488.1	0.9	0.78	0.27
						42	3802.0	1495.6	1.2	0.37	0.15

TABLE IV. γ-ray spectrum up to 1.5 MeV from thermal-neutron capture by ^{234}U.

Number	E_γ (keV)	dE_γ (keV)	I_γ ($\gamma/10^2 n$)	dI_γ ($\gamma/10^2 n$)	Number	E_γ (keV)	dE_γ (keV)	I_γ ($\gamma/10^2 n$)	dI_γ ($\gamma/10^2 n$)
1	23.45	0.05	0.04	0.015	51	376.35	0.09	0.35	0.07
2	29.86	0.05	0.02	0.01	52	378.83	0.16	0.10	0.05
3	30.90	0.10	0.01	0.005	53	380.01	0.08	1.9	0.4
4	38.72	0.06	0.01	0.005	54	392.95	0.09	2.3	0.5
5	42.14	0.05	0.03	0.01	55	399.29	0.11	0.15	0.06
6	46.16	0.05	0.02	0.005	56	412.31	0.12	0.24	0.08
7	47.60	0.05	0.03	0.01	57	413.58	0.09	0.90	0.20
8	51.67	0.05	0.03	0.01	58	422.53	0.11	0.15	0.07
9	53.51	0.15	0.01	0.005	59	445.83	0.13	0.21	0.04
10	54.06	0.06	0.01	0.005	60	454.56	0.20	0.09	0.04
11	77.61	0.05	0.16	0.04	61	478.11	0.11	0.42	0.08
12	89.90	0.05	0.02	0.01	62	491.14	0.11	0.39	0.07
13	116.25	0.04	0.26	0.05	63	495.92	0.30	0.05	0.02
14	119.38	0.06	0.01	0.005	64	504.8	0.1	0.32	0.08
15	121.95	0.06	0.03	0.01	65	517.0	0.3	0.06	0.02
16	123.23	0.06	0.02	0.01	66	558.3	0.1	0.12	0.03
17	124.97	0.28	0.005	0.005	67	564.1	0.2	0.05	0.02
18	129.26	0.03	3.3	0.7	68	582.6	0.1	0.30	0.06
19	132.18	0.05	0.02	0.01	69	586.4	0.1	0.20	0.04
20	140.71	0.13	0.01	0.005	70	595.8	0.2	0.20	0.05
21	141.64	0.09	0.02	0.007	71	599.2	0.1	0.52	0.11
22	142.18	0.08	0.02	0.007	72	602.4	0.8	0.05	0.02
23	146.65	0.07	0.02	0.005	73	608.4	0.2	0.13	0.03
24	148.14	0.13	0.01	0.005	74	612.6	0.1	0.35	0.07
25	159.15	0.14	0.02	0.01	75	615.2	0.4	0.12	0.05
26	161.39	0.05	0.12	0.003	76	616.9	0.2	0.46	0.11
27	167.13	0.09	0.03	0.01	77	618.4	0.1	0.72	0.16
28	171.56	0.10	0.03	0.01	78	621.8	0.7	0.04	0.02
29	172.56	0.08	0.04	0.02	79	624.7	0.1	0.87	0.18
30	174.96	0.12	0.03	0.01	80	627.4	1.1	0.02	0.02
31	181.51	0.14	0.02	0.01	81	633.1	0.1	1.9	0.4
32	182.76	0.13	0.01	0.005	82	637.8	0.1	3.4	0.7
33	184.03	0.11	0.02	0.01	83	640.4	0.2	0.23	0.06
34	195.67	0.06	0.10	0.03	84	642.6	0.5	0.07	0.03
35	197.02	0.08	0.05	0.02	85	646.0	0.1	1.3	0.3
36	203.45	0.06	0.55	0.10	86	649.5	0.3	0.20	0.05
37	212.42	0.11	0.04	0.02	87	651.9	0.1	1.2	0.3
38	218.48	0.07	0.05	0.02	88	654.4	0.3	0.14	0.04
39	229.05	0.13	0.05	0.03	89	658.9	0.1	0.87	0.19
40	263.71	0.07	0.20	0.005	90	664.4	0.2	0.64	0.15
41	316.27	0.08	0.28	0.06	91	670.7	0.4	0.18	0.08
42	320.51	0.17	0.03	0.01	92	680.0	0.2	0.14	0.03
43	323.54	0.12	0.14	0.05	93	685.9	0.1	0.50	0.10
44	332.65	0.08	0.41	0.10	94	691.0	0.1	0.28	0.06
45	341.34	0.08	0.35	0.08	95	694.0	0.2	0.24	0.05
46	344.83	0.10	0.35	0.08	96	698.3	0.3	0.15	0.04
47	367.15	0.17	0.11	0.04	97	700.3	0.3	0.21	0.05
48	371.10	0.16	0.08	0.04	98	703.7	0.1	0.68	0.14
49	373.74	0.16	0.07	0.04	99	714.4	0.1	0.45	0.10
50	374.94	0.08	1.1	0.2	100	718.2	0.1	0.56	0.11

TABLE IV *(Continued)*

Number	E_γ (keV)	dE_γ (keV)	I_γ ($\gamma/10^2 n$)	dI_γ ($\gamma/10^2 n$)	Number	E_γ (keV)	dE_γ (keV)	I_γ ($\gamma/10^2 n$)	dI_γ ($\gamma/10^2 n$)
101	724.3	0.4	0.04	0.02	151	955.6	0.2	0.50	0.10
102	728.2	0.2	0.12	0.03	152	962.2	0.3	0.07	0.02
103	733.5	0.6	0.04	0.02	153	965.3	0.3	0.10	0.03
104	735.7	0.1	0.31	0.07	154	968.4	0.2	0.38	0.08
105	741.7	0.3	0.08	0.02	155	969.9	0.2	0.23	0.06
106	747.9	0.1	1.1	0.2	156	977.2	0.3	0.17	0.05
107	750.8	0.3	0.10	0.02	157	978.9	0.7	0.10	0.03
108	756.6	0.1	0.21	0.04	158	981.2	0.5	0.12	0.03
109	760.9	0.2	0.13	0.03	159	983.2	0.3	0.10	0.03
110	762.9	0.3	0.10	0.03	160	987.0	0.2	0.37	0.08
111	766.7	0.2	0.19	0.04	161	990.2	0.2	0.61	0.12
112	769.7	0.1	1.8	0.4	162	992.8	0.2	0.27	0.06
113	775.9	0.2	0.11	0.02	163	995.4	0.2	0.23	0.05
114	779.4	0.1	0.20	0.04	164	1000.0	0.6	0.04	0.02
115	784.0	0.5	0.06	0.02	165	1002.2	0.2	0.34	0.08
116	787.0	0.1	0.39	0.08	166	1005.8	0.5	0.04	0.02
117	792.5	0.2	0.26	0.05	167	1009.2	0.3	0.10	0.03
118	799.0	0.2	0.20	0.04	168	1015.9	0.2	0.25	0.05
119	803.4	0.4	0.11	0.03	169	1019.8	0.2	0.18	0.04
120	805.5	0.2	0.33	0.07	170	1024.7	0.6	0.06	0.02
121	808.4	0.3	0.14	0.04	171	1028.1	0.9	0.02	0.02
122	813.5	0.1	0.55	0.11	172	1032.7	0.2	0.15	0.03
123	821.3	0.2	0.12	0.03	173	1045.0	0.2	0.33	0.07
124	823.6	0.2	0.08	0.02	174	1047.5	0.2	0.26	0.06
125	828.9	0.1	0.17	0.04	175	1057.3	0.2	0.17	0.04
126	832.3	0.1	0.19	0.04	176	1060.1	0.3	0.10	0.03
127	840.3	0.2	0.17	0.04	177	1072.6	0.2	0.29	0.06
128	843.7	0.1	0.57	0.11	178	1078.2	0.6	0.07	0.02
129	847.1	0.2	0.08	0.02	179	1083.1	0.4	0.05	0.02
130	849.9	0.3	0.08	0.02	180	1085.8	0.2	0.13	0.03
131	852.4	0.2	0.26	0.05	181	1090.9	0.2	0.14	0.03
132	856.7	0.3	0.06	0.02	182	1095.6	0.2	0.18	0.04
133	863.8	0.2	0.14	0.04	183	1099.0	0.3	0.10	0.03
134	878.7	0.2	0.20	0.04	184	1102.9	0.7	0.03	0.02
135	886.0	0.5	0.02	0.01	185	1104.8	0.4	0.06	0.02
136	889.5	0.2	0.26	0.05	186	1111.4	0.3	0.07	0.02
137	892.3	0.2	0.12	0.03	187	1115.6	0.3	0.07	0.02
138	894.6	0.5	0.04	0.02	188	1117.7	0.5	0.05	0.02
139	901.1	0.3	0.06	0.02	189	1124.4	0.3	0.07	0.02
140	905.0	0.2	0.12	0.03	190	1142.2	0.2	0.58	0.12
141	911.8	0.2	0.10	0.03	191	1145.0	0.3	0.08	0.02
142	916.2	0.4	0.05	0.02	192	1149.9	0.5	0.03	0.02
143	918.2	0.3	0.10	0.03	193	1153.2	0.5	0.04	0.02
144	927.8	0.2	0.12	0.03	194	1157.0	0.3	0.09	0.03
145	931.1	0.3	0.05	0.02	195	1161.8	0.7	0.04	0.02
146	938.9	0.8	0.07	0.04	196	1164.8	0.3	0.16	0.04
147	941.2	0.7	0.08	0.04	197	1167.7	0.5	0.08	0.03
148	944.9	0.4	0.12	0.04	198	1170.6	1.1	0.03	0.02
149	949.2	0.2	0.67	0.14	199	1173.0	0.2	0.21	0.05
150	950.9	0.2	0.70	0.15	200	1177.0	0.8	0.07	0.03

TABLE IV *(Continued)*

Number	E_γ (keV)	dE_γ (keV)	I_γ ($\gamma/10^2 n$)	dI_γ ($\gamma/10^2 n$)	Number	E_γ (keV)	dE_γ (keV)	I_γ ($\gamma/10^2 n$)	dI_γ ($\gamma/10^2 n$)
201	1182.9	0.5	0.05	0.02	236	1331.4	0.3	0.17	0.04
202	1185.5	0.2	0.27	0.06	237	1333.9	0.5	0.10	0.03
203	1190.2	0.6	0.03	0.01	238	1337.1	0.2	0.25	0.05
204	1194.2	0.2	0.24	0.05	239	1344.5	0.3	0.11	0.03
205	1197.5	0.3	0.10	0.03	240	1349.7	0.5	0.07	0.02
206	1202.5	0.3	0.09	0.03	241	1354.4	0.3	0.19	0.04
207	1206.0	0.8	0.04	0.02	242	1357.9	0.2	0.42	0.09
208	1210.5	0.7	0.04	0.02	243	1364.1	0.7	0.06	0.03
209	1213.0	0.5	0.06	0.02	244	1367.1	0.6	0.12	0.04
210	1220.6	0.2	0.20	0.04	245	1369.3	0.5	0.18	0.05
211	1224.4	0.3	0.18	0.05	246	1372.0	1.0	0.08	0.03
212	1226.6	0.5	0.14	0.04	247	1377.4	0.4	0.09	0.03
213	1229.9	0.8	0.05	0.02	248	1382.5	0.2	0.40	0.08
214	1233.1	0.2	0.35	0.07	249	1386.9	0.4	0.11	0.03
215	1238.1	0.6	0.05	0.02	250	1391.3	0.3	0.28	0.06
216	1245.4	0.3	0.14	0.07	251	1393.9	0.7	0.10	0.03
217	1246.4	0.3	0.23	0.08	252	1397.2	0.7	0.10	0.04
218	1252.4	0.3	0.14	0.04	253	1399.9	0.3	0.23	0.06
219	1256.0	0.3	0.05	0.02	254	1412.7	0.2	0.24	0.05
220	1265.4	0.2	0.17	0.04	255	1416.9	0.6	0.05	0.02
221	1269.0	0.2	0.18	0.04	256	1422.9	0.4	0.08	0.03
222	1272.3	0.5	0.08	0.02	257	1425.6	0.3	0.19	0.05
223	1279.8	0.2	0.08	0.02	258	1428.0	0.5	0.06	0.02
224	1283.6	0.2	0.25	0.05	259	1435.9	0.3	0.09	0.03
225	1286.1	0.7	0.04	0.01	260	1438.3	0.2	0.16	0.04
226	1289.8	0.4	0.05	0.02	261	1442.9	0.4	0.04	0.02
227	1293.6	0.2	0.47	0.10	262	1449.0	0.4	0.13	0.04
228	1296.7	0.2	0.19	0.04	263	1450.9	0.4	0.07	0.03
229	1301.3	0.2	0.28	0.06	264	1461.6	0.3	0.16	0.04
230	1304.8	0.3	0.09	0.03	265	1464.3	0.3	0.18	0.04
231	1308.1	0.2	0.28	0.06	266	1468.3	0.5	0.08	0.03
232	1318.2	0.3	0.11	0.04	267	1470.4	0.8	0.04	0.02
233	1319.6	0.4	0.13	0.04	268	1473.1	0.8	0.03	0.02
234	1324.3	0.3	0.09	0.03	269	1477.9	0.3	0.18	0.04
235	1328.8	0.9	0.05	0.02	270	1480.8	0.7	0.05	0.02
					271	1484.3	0.7	0.06	0.02
					272	1493.7	0.4	0.09	0.03
					273	1496.2	0.5	0.08	0.03

anism, populate preferentially states of $J = \frac{1}{2}$ or $\frac{3}{2}$. Thus high-energy γ rays are a great aid in locating band heads for $K = \frac{1}{2}$ and $\frac{3}{2}$ bands. A third class of information used for the location of rotational bands comes from the reaction ^{233}U(t, p). In the present work it is found that in addition to the target ground-state configuration the (t, p) reaction preferentially excites states whose decay properties indicate that they bear a close relationship to the target ground-state configuration. The single-particle or single-hole states that are strongly excited in the (d, p) and (d, t) reactions are not excited measurably by the (t, p) reaction.

Using the tools described above, as many as possible of the levels observed in the charged-particle reactions are assigned to rotational bands. The major inputs to the initial assignments are the rotational level spacings, the measured l values where available, and the primary (n, γ) results. Then the assignments are further checked by sorting out the low-energy (n, γ) results and requiring that the observed lines connect levels with reasonable spin changes.

The (d, p) and (d, t) angular distributions have been used to extract occupation probabilities (U^2 and V^2) for each band and spectroscopic strengths (the experimental equivalent of the Nilsson expansion coefficients) for members of

TABLE V. Experimental characteristics of rotational bands of ^{235}U determined in the present experiment. Theoretical spectroscopic factors are included for comparison.

Band	Energy (keV)	$\hbar^2/2$ (keV)	a	U^2	V^2		$\frac{1}{2}$	$\frac{3}{2}$	$\frac{5}{2}$	$\frac{7}{2}$	$\frac{9}{2}$	$\frac{11}{2}$	$\frac{13}{2}$	$\frac{15}{2}$	Sum
$\frac{7}{2}^-[743]$ [a]	0.0	5.14		0.56	0.44	A^2(Expt.)						0.069	d	1.06	1.13
						C^2(Rost)						0.139		0.775	0.91
						C^2(Nilsson)						0.078		0.918	1.00
$\frac{1}{2}^+[631]$ [a]	0.08	6.16	−0.284	0.76	0.24	A^2(Expt.)	0.044	0.242	0.006	0.098	0.306	0.096			0.79
						C^2(Rost)	0.162	0.323	0.009	0.036	0.185	0.227			0.94
						C^2(Nilsson)	0.122	0.310	0.016	0.092	0.204	0.234			0.98
$\frac{5}{2}^+[622]$ [a]	129.26	6.01		0.80	0.20	A^2(Expt.)			0.031	0.016	0.454	0.276			0.78
						C^2(Rost)			0.098	0.004	0.555	0.222			0.88
						C^2(Nilsson)			0.058	<0.001	0.653	0.224			0.94
$\frac{5}{2}^+[633]$ [a]	332.7	4.94		0.31	0.69	A^2(Expt.)			0.006	0.054	0.056				0.12
						C^2(Rost)			0.030	0.169	0.112				0.31
						C^2(Nilsson)			0.019	0.123	0.132				0.27
$\frac{3}{2}^+[631]$ [a]	393.0	6.72		0.24	0.76	A^2(Expt.)		0.019	0.095	0.060	0.114	0.004	0.048		0.34
						C^2(Rost)			0.204	0.039	0.383	0.259	0.095		0.98
						C^2(Nilsson)		0.009	0.139	0.021	0.420	0.334	0.084		1.00
$\frac{7}{2}^+[624]$ [b]	491.9	4.62		0.95	0.05	A^2(Expt.)				0.005	d	0.167			0.17
						C^2(Rost)				0.068	0.073	0.810			0.88
						C^2(Nilsson)				0.043	0.089	0.835			0.88
$\frac{5}{2}^+[\,?\,]$ [b]	507.7	6.23		0.81	0.19	A^2(Expt.)			0.049	0.023	0.053				0.13
$\frac{5}{2}^-[752]$ [b]	633.1	5.43													
$\frac{3}{2}^-[\,?\,]$	637.1														
$\frac{1}{2}^+[\,?\,]$ [c]	640.4	4.47	−0.14	0.81	0.19										0.05
$\frac{1}{2}^-[501]$ $+\frac{1}{2}^-[770]$	659.0	4.48	2.34	0.09	0.91	A^2(Expt.)	0.143	0.050	0.014	0.012	0.012	0.216	0.048		0.50
						$C^2(R, \beta=0.245)$	0.558	0.104	0.126	<0.001	0.007	0.034			0.83
						$C^2(R, \beta=0.240)$	0.306	0.062	0.068	0.002	0.003	0.102			0.54
$\frac{1}{2}^+[\,?\,]$ [b]	760.9	5.04	−0.417	0.53	0.47	A^2(Expt.)	0.023	0.045	0.041	0.064					0.17
$\frac{3}{2}^+[\,?\,]$ [c]	843.7	5.53		0.95	0.05	A^2(Expt.)		0.028	0.010	0.021	0.222				0.28
						A^2(Negative) [e]		0.019	0.020	0.019	0.330				0.39
$\frac{1}{2}^-[\,?\,]$ [b]	878.7	5.12	−0.128	0.86	0.14	A^2(Expt.)	0.036	0.041	0.056	0.051					0.18
$\frac{7}{2}^+[624]$ [b]	970.0	6.68		0.90	0.10	A^2(Expt.)				0.006	0.171	0.621			0.80
$\frac{1}{2}^+[\,?\,]$ [b]	992.8	4.90	−0.350	0.33	0.67	A^2(Expt.)	0.029	0.039	0.139	0.061					0.32
$\frac{1}{2}^+[\,?\,]$ [b]	1072.7	7.09	0.240	0.41	0.59	A^2(Expt.)	0.015	0.004	0.040	0.092					0.15
$\frac{5}{2}^+[\,?\,]$ [b]	1116.2	5.87		0.62	0.38	A^2(Expt.)			(0.010)	0.036	0.081				0.13
$\frac{1}{2}^-[761]$ [b]	1194.3	4.43	−0.369	0.92	0.08	A^2(Expt.)	0.033	0.028	0.065	0.154	0.085	0.298			0.66
						C^2(Rost)	0.002	0.016	0.009	0.368	0.014	0.451			0.86
						C^2(Nilsson)	0.022	0.086	0.059	0.246	0.108	0.210			0.73

TABLE V (*Continued*)

Band	Energy (keV)	$\hbar^2/2$ (keV)	a	U^2	V^2		$\frac{1}{2}$	$\frac{3}{2}$	$\frac{5}{2}$	$\frac{7}{2}$	$\frac{9}{2}$	$\frac{11}{2}$	$\frac{13}{2}$	$\frac{15}{2}$	Sum
$\frac{3}{2}^-[?]$ [b]	1242.3	9.03		0.89	0.11	A^2(Expt.)	0.045	0.046	0.025	0.168	0.179				0.46
$\frac{1}{2}^+[620]$ [a]	1273.0	6.51	0.253	0.93	0.07	A^2(Expt.)	0.150	0.038	0.173	(0.060)	0.210				0.63
						C^2(Rost)	0.160	0.081	0.201	0.174	0.202				0.82
						C^2(Nilsson)	0.139	0.031	0.253	0.256	0.193				0.87
$\frac{1}{2}^-[750]$ [b]	1382.5	5.97	0.222	0.97	0.03	A^2(Expt.)	0.029	0.041	0.061	0.074	0.120	0.038			0.36
						C^2(Rost)	0.027		0.152	0.012	0.333	0.012			0.52
						C^2(Nilsson)	<0.001	0.017	0.029	0.103	0.186	0.134			0.47
$\frac{3}{2}^+[622]$ [b]	1412.8	5.16		0.95	0.05	A^2(Expt.)	0.035	0.018	0.022	0.042					0.12
						C^2(Rost)	0.231	0.108	0.284	0.155					0.78
						C^2(Nilsson)	0.162	0.091	0.430	0.129					0.81

[a] Firm assignments.
[b] Probable assignments.
[c] Reasonable assignments.
[d] State was obscured in charged-particle results.
[e] Values obtained for A^2 if this band is assumed to have negative parity.

each band. These calculations use the following relations[1]:

$$\frac{d\sigma}{d\omega}(d,p) = 3A^2U^2\Phi_l(\theta), \tag{1}$$

$$\frac{d\sigma}{d\omega}(d,t) = 6.67A^2V^2\Phi_l(\theta), \tag{2}$$

where A^2 is the experimental spectroscopic strength and the angular distributions $\Phi_l(\theta)$ are calculated with the code[9] JULIE using parameters determined from elastic scattering as described in the Appendix. If it is assumed that the occupation probabilities do not depend strongly on the mass of the target nucleus then the relation:

$$U^2 + V^2 = 1$$

can be used and U^2, V^2, and A^2 determined for cases where a level is observed by both (d,p) and (d,t) reactions. A further check on the rotational-band assignments is obtained from the requirement that U^2 and V^2 must be the same for all members of a given band.

The details of the assignments will be presented in the remainder of this section. Because of the bulk of data involved, each rotational band will be treated separately, with the relevant information presented in Table V and in Figs. 5–11. As has been implied above, the confidence which can be placed in a particular band assignment depends on the amount of supporting evidence. The level of confidence has been indicated in Table V by the superscript a, b, or c on the band assignment, with a representing firm assignments, b probable assignments, and c reasonable possibilities.

The population of levels in particular bands by (d,p), (d,t), (t,p), (d,d'), and (n,γ) reactions is indicated in the appropriate figure. A key for coding of the various excitation modes for each level in Figs. 5–11 is given in Fig. 5. In addition, many of the low-lying levels of ^{235}U have also been observed in radioactive decay,[13] Coulomb excitation,[14] and (^{3}He, α) reactions.[15] Many of the (d,p) and (d,t) excitations were also identified by the Argonne group,[7] and in general the agreement is good. The γ-ray deexcitation of levels of a particular band is also indicated in Figs. 5–11.

The measured values of U^2 and V^2 and the measured spectroscopic strengths (A^2) are given in Table V. If the relative values of A^2 suggest that a particular Nilsson assignment is called for, two sets of Nilsson coefficients (C^2) are included for comparison. The first set is always from the Rost[16] coupled-channel calculation in a Woods-Saxon well; the second set is from a Nilsson harmonic-oscillator calculation by Udagawa.[17] A deformation of $\beta = 0.25$ is assumed in both cases.

The well parameters for the Woods-Saxon calculation are those used by Rost to fit the levels in ^{209}Pb.[18]

A. $\frac{7}{2}^-[743]$

The $\frac{7}{2}^-[743]$ band (Fig. 5) was previously known to be the ground-state rotational band of ^{235}U.[13] The $\frac{7}{2}^-$ member lies only 80 eV below a $\frac{1}{2}^+$ state, and is predicted to have a vanishingly small spectroscopic strength. Thus the $\frac{7}{2}^-$ state is not observed in the (d, p) or (d, t) reactions. The $\frac{9}{2}^-$ member of the band is also predicted to have a very small spectroscopic strength, and although a few scattered tracks were found at the correct excitation energy in the (d, p) and (d, t) data, no measurement of the spectroscopic strength could be reliably made. The excitation energy of this $\frac{9}{2}^-$ state is known accurately, since its γ decay was observed. The $\frac{13}{2}^-$ member is unresolved from the $\frac{7}{2}^+$ member of the $\frac{5}{2}^+[622]$ band. The $\frac{15}{2}^-$ member of the band is clearly observed in the (d, p) and (d, t), and probably in the (d, d') reactions; it is also observed in the $(^3\mathrm{He}, \alpha)$ reaction.[15]

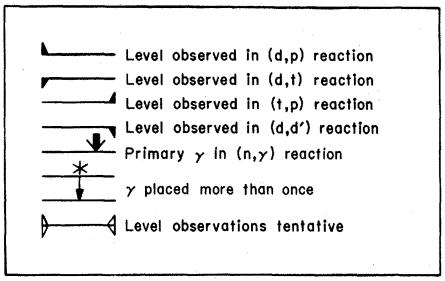

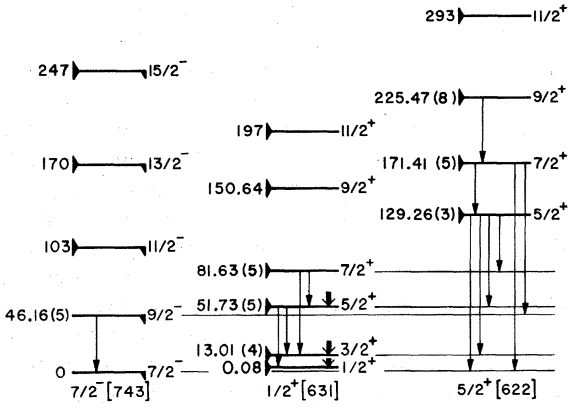

FIG. 5. States identified in the $\frac{7}{2}^-[743]$, $\frac{1}{2}^+[631]$, and $\frac{5}{2}^+[622]$ bands. Low-energy γ-ray deexcitations which were observed are indicated. Parentheses enclose probable errors in the last digit for the positions in keV of levels for which γ-ray deexcitations were observed. Probable errors in the excitations of other states are indicated in Table I.

B. $\frac{1}{2}^+[631]$

The band head of the $\frac{1}{2}^+[631]$ band (Fig. 5) lies at 80 eV.[13] Members of the band up to the $\frac{11}{2}^+$ state are observed in the (d, p) and (d, t) reactions. This band has been previously observed, both in the α decay[13] of ^{239}Pu and the work of the Argonne group.[7] Deexcitation of the $\frac{9}{2}$ member was not observed in the (n, γ) experiment because the expected transitions were obscured by the U $K\alpha_1$ x-ray line and a contaminating Au $K\alpha_1$ x-ray line.

C. $\frac{5}{2}^+[622]$

The $\frac{7}{2}^+$ member of the $\frac{5}{2}^+[622]$ band (Fig. 5) cannot be separated in the present work from the $\frac{13}{2}^-$ member of the $\frac{7}{2}^-[743]$ band. The value of A^2 given in the table may therefore be somewhat too large due to the inclusion of the unresolved $\frac{13}{2}^-$ state. This effect is not serious because the cross section for the $\frac{7}{2}^+$ state should be much larger than that for the $\frac{13}{2}^-$ state. The assignment is in agreement with previous work.[7]

D. $\frac{5}{2}^+[633]$

The $\frac{5}{2}^+[633]$ band (Fig. 6) is the ground-state band of ^{233}U. It should therefore be strongly populated in the reaction $^{233}\mathrm{U}(t, p)^{235}\mathrm{U}$, and the $\frac{5}{2}^+$

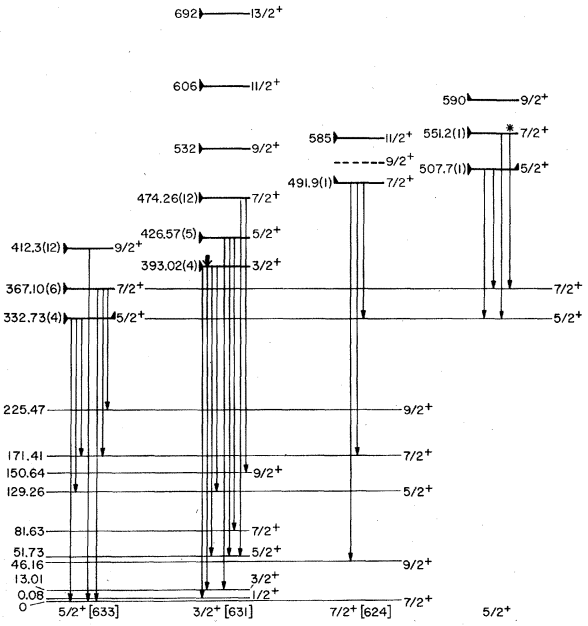

FIG. 6. States identified in the $\frac{5}{2}^+[633]$, $\frac{3}{2}^+[631]$, $\frac{7}{2}^+[624]$, and the $\frac{5}{2}^+$ at 507.7-keV bands. For further details refer to the legend for Fig. 5.

state is the strongest excitation observed in the (t, p) spectrum. The (d, p) and (d, t) reactions indicate that the single-particle strength of the band is a factor of 2 lower than predicted.

E. $\frac{3}{2}^+[631]$

All members of the $\frac{3}{2}^+[631]$ band (Fig. 6) have been observed up to the $\frac{13}{2}^+$ state. The $\frac{3}{2}^+$ member is populated by a weak direct transition in the ^{234}U(n, γ) reaction and the decay of the first three members is observed. This band had previously been observed through the $\frac{9}{2}^+$ member in the α decay of ^{239}Pu.[13] The band contains only one third of its predicted single-particle strength. It should be noted, however, that the measured A^2 for the $\frac{11}{2}^+$ state is anomalously small. The factor of approximately 20 which would be required to bring the measured A^2 into better relative agreement with theory is far larger than any expected experimental error.

F. $\frac{7}{2}^+[624]$

The experimental evidence for the $\frac{7}{2}^+[624]$ band (Fig. 6) is somewhat scanty, since the $\frac{9}{2}^+$ member is believed to be obscured by the $\frac{9}{2}^+$, $\frac{3}{2}^+[631]$ state. The three γ rays which depopulate the 491.9-keV state suggest that its spin is $\frac{7}{2}$. The relative spectroscopic strengths of the $\frac{7}{2}^+$ and $\frac{11}{2}^+$ members would then be in reasonable agreement with the Nilsson predictions, although the measured single-particle strength is some five times smaller than predicted for the $\frac{7}{2}^+[624]$ band.

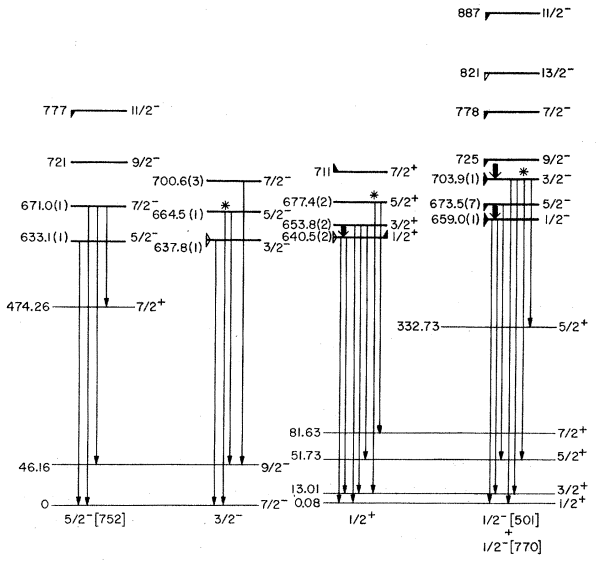

FIG. 7. States identified in the $\frac{5}{2}^-[752]$, $\frac{3}{2}^-$ at 637.8-keV, $\frac{1}{2}^+$ at 640.5-keV, and $\frac{1}{2}^-[501] + \frac{1}{2}^-[770]$ bands. For further details refer to the legend for Fig. 5.

G. $\frac{5}{2}^+$ at 507.7 keV

Since the bandhead of the $\frac{5}{2}^+$ band at 507.7 keV (Fig. 6) is populated in the reaction ^{233}U$(t,p)^{235}$U, it is likely to be composed partly of a particle-plus-phonon state based on the $\frac{5}{2}^+[633]$ band. This interpretation is supported by the observed decay of both the $\frac{5}{2}^+$ and $\frac{7}{2}^+$ members to members of the $\frac{5}{2}^+[633]$ band. The 507.7-keV state has a measured $l_n = 2$ angular distribution in the (d,p) reaction and is observed to decay to $\frac{5}{2}^+$ and $\frac{7}{2}^+$ states in the (n, γ) reaction supporting the assignment of $J^\pi = \frac{5}{2}^+$.

H. $\frac{5}{2}^-[752]$

Stephens *et al.*[14] have observed through Coulomb excitation a band beginning at 633 keV to which they propose an assignment of $\frac{5}{2}^-[752]$ (Fig. 7). The $\frac{15}{2}^-$ member has been observed in the $(^3$He, $\alpha)$ reaction.[15] Almost no information is available from the charged-particle reactions of the present work although a state at 777 keV, corresponding in energy to the $\frac{11}{2}^-$ member,[14] may be excited in the (d, t) reaction, but it is degenerate in energy with the $\frac{7}{2}^-$ member of the band we propose in Sec. J. The predicted spectroscopic strength lies predominantly in the $\frac{15}{2}^-$ member. The observed decay is primarily to members of the ground-state band.

I. $\frac{3}{2}^-$ at 637.8 keV

Stephens *et al.*[14] have suggested that the band observed in Coulomb-excitation experiments beginning at 637.8 keV (Fig. 7) is the $K-2$ γ vibration based on the ground state. Our (d,p) spectra show a state at 639 ± 2 keV with angular distribution characteristic of $l_n = 1$, in agreement with the proposed $\frac{3}{2}$ bandhead assignment. We observe γ decay to members of the ground-state band which is also consistent with the previous assignment.

J. $\frac{1}{2}^+$ at 640.5 keV

Since the band head of this $\frac{1}{2}^+$ band (Fig. 7) is populated in the reaction ^{233}U$(t,p)^{235}$U, it may be in part a 2^+ phonon state built on the $\frac{5}{2}^+[633]$ band. The state seen at 639 keV with $l_n = 1$ in the (d,p) reaction is assigned to the $\frac{3}{2}^-$ band (see Sec. III above) and obscures the $\frac{1}{2}^+$ state assigned to this band. Unfortunately, two other levels in this band are also obscured in the (d,p) and (d, t) reactions by other states at 659 and 675 keV. The band appears to decay primarily to the $\frac{1}{2}^+[631]$ band and may contain part of its strength.

K. $\frac{1}{2}^-[501]+\frac{1}{2}^-[770]$

The $\frac{1}{2}^-$ band presented in Fig. 7 can best be explained as a mixture of the $\frac{1}{2}^-[501]$ and of the $\frac{1}{2}^-[770]$ Nilsson states. The decoupling parameter (+2.34) is an anomalous one, since for the $\frac{1}{2}^-[501]+\frac{1}{2}^-[770]$ mixture a negative decoupling parameter is expected. However, attempts to group the $\frac{1}{2}^-$ and $\frac{3}{2}^-$ states with levels other than those in Fig. 7 results in an unacceptable value for $\hbar^2/2I$. This extreme value could be obtained as a result of strong Coriolis coupling with other bands, but this has been shown to be very improbable in a Coriolis calculation by Bunker.[19] It is possible that a significant particle+phonon admixture in the band could explain the decoupling parameter,[20] because of interference terms involving the $\frac{1}{2}^-[501]+\frac{1}{2}^-[770]$ band and the $\frac{1}{2}^+[631]$ band.

The spins and parities of the 659.0- and 703.8-keV states are assigned on firm grounds. Both have measured $l_n=1$ angular momenta. The 659.0-keV state decays to states of spin $\frac{1}{2}$ and $\frac{3}{2}$, while the 703.9-keV state is not only populated by a direct transition, but decays to states of spin $\frac{1}{2}$, $\frac{3}{2}$, and $\frac{5}{2}$. All of these considerations confirm the assigned spins and parities of these two states.

The spectroscopic strengths support a $\frac{1}{2}^-[770]+\frac{1}{2}^-[501]$ assignment. The $\frac{1}{2}^-[501]$ band has a strong $\frac{1}{2}^-$ component, with decreasing strength in states of higher spin. The $\frac{1}{2}^-[770]$ band has almost no strength in the low-spin states, but has its strength in the $\frac{11}{2}^-$ and $\frac{15}{2}^-$ states. The standard Nilsson calculation does not have terms in the Hamiltonian which will include contributions from two different oscillator shells. In the Rost calculations,[16] however, this problem never arises, and the "$\Delta N=2$" mixing calculation is straightforward. Since the results are very sensitive to the deformation used, Table V includes Rost calculations for two values of β differing by $\Delta\beta=0.005$. The calculation for $\beta=0.240$ resembles the experimental results. The extreme sensitivity to β is probably unphysical, since "zero-point oscillations" in β are expected.

The $\frac{11}{2}^-$ and $\frac{15}{2}^-$ members of this band should have been observed in the (^{3}He, α) results.[15] The state observed at 884 ± 4 keV has the appropriate energy and intensity to be the $\frac{11}{2}$ member. The state observed at 1090 ± 5 keV has an intensity and probable l value consistent with the $\frac{15}{2}^-$ member of this band, but its position is considerably removed from the value of 1036 keV predicted by the $\hbar^2/2I$ and decoupling parameter values given in Table V.

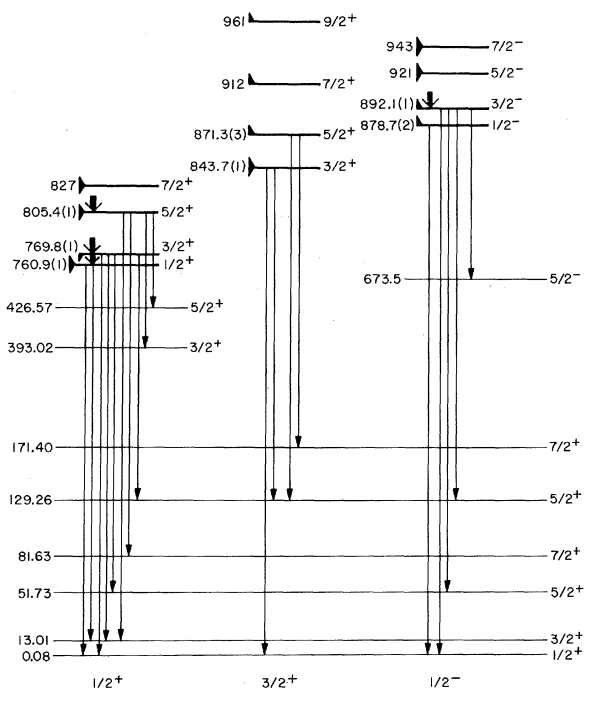

FIG. 8. States identified in the $\frac{1}{2}^+$ at 760.9-, $\frac{3}{2}^+$ at 843.7-, and $\frac{1}{2}^-$ at 878.7-keV bands. For further details refer to the legend for Fig. 5.

L. $\frac{1}{2}^+$ Band at 760.9 keV

The $\frac{1}{2}^+$ band at 760.9 keV (Fig. 8) is interesting in that U^2 is approximately equal to V^2. It is probably a mixture of particle and hole states through phonon interactions. It is difficult to associate this band with any of the Nilsson configurations. The $\frac{5}{2}^+$ state is weakly populated by a direct $E2$ transition from the capture state. The suggested $\frac{1}{2}^+$ and $\frac{3}{2}^+$ states are also populated by high-energy transitions. The observed decay modes of the $\frac{1}{2}^+$, $\frac{3}{2}^+$, and $\frac{5}{2}^+$ states confirm their spin assignments.

M. $\frac{3}{2}^+$ Band at 843.7 keV

The parity of the $\frac{3}{2}^+$ band at 843.7 keV (Fig. 8) is not well determined. The angular distribution for the 843.7 state allows either $l_n=1$ or 2. Table V contains values of A^2 for both parities.

N. $\frac{1}{2}^-$ Band at 878.7 keV

The existence of the $\frac{1}{2}^-$ band at 878.7 keV (Fig. 8) is suggested by a high-energy transition to the 892.1-keV state, and by the measured $l_n=3$ for the 943-keV state. The band head decays by an observed 878.7-keV γ, although a branching transition to the $\frac{3}{2}^+$ member of the $\frac{1}{2}^+[631]$ band is not seen.

O. $\frac{7}{2}^+$ Band at 970.0 keV

The ^{235}U$(d, d')^{235}$U reaction populates the band head of a $\frac{7}{2}^+$ band at 970.0 keV (Fig. 9) and it may therefore be part octupole vibration based on the $\frac{7}{2}^-[743]$ ground-state band. The relative spectroscopic strengths resemble those of the $\frac{7}{2}^+[624]$ band and thus the band may contain a large part of the $\frac{7}{2}^+[624]$ strength. The band head spin and mixed configurational assignment is also suggested by the observed γ decay of the state.

P. $\frac{1}{2}^+$ Band at 992.7 keV

The $\frac{1}{2}^+$ band at 992.7 keV (Fig. 9) is a possible candidate for $\frac{1}{2}^+[640]$ assignment; it cannot be simply the $\frac{1}{2}^+[640]$ band, however, since the occupation probabilities indicate that some particle strength has been mixed into what should be almost a pure hole state ($V^2 \approx 1$). The $\frac{5}{2}^+$ state is populated by a weak $E2$ transition in the high-energy (n, γ) spectrum, in addition to the states assigned as $\frac{1}{2}^+$ and $\frac{3}{2}^+$.

Q. $\frac{1}{2}^+$ Band at 1072.9 keV

The $\frac{1}{2}^+$ band at 1072.9 keV (Fig. 9) presents another case of anomalous values for U^2 and V^2. The small spectroscopic strength of the band implies a predominantly particle + phonon character. The $\frac{1}{2}^+$ and $\frac{3}{2}^+$ states are populated by primary transitions in the (n, γ) reaction.

R. $\frac{5}{2}^+$ Band at 1116.2 keV

The reaction ^{233}U$(t, p)^{235}$U populates the band head of a $\frac{5}{2}^+$ band at 1116.2 keV (Fig. 10). It may, therefore contain a component generated by the coupling of a 0^+ phonon to the $\frac{5}{2}^+[633]$ band. The band decays to members of the ground state and the $\frac{5}{2}^+[622]$ band as well as to the $\frac{5}{2}^+$ level of the $\frac{5}{2}^+[633]$ band.

S. $\frac{1}{2}^-[761]$

The band presented in Fig. 10 is believed to have the $\frac{1}{2}^-[761]$ assignment, even though the measured spectroscopic strength of the $\frac{9}{2}^-$ state is too large. The measured spectroscopic strength for the entire band suggests that it is a reasonably pure single-particle state. The suggested assignment is supported by measured $l_n = 1$ angular momentum transfers for the $\frac{1}{2}^-$ and $\frac{3}{2}^-$ states. The $\frac{1}{2}^-$ state is populated by a primary transition in the (n, γ) reaction. The $\frac{11}{2}^-$ member at 1364 keV may have been observed in the (^{3}He, α) experiments.[15] In

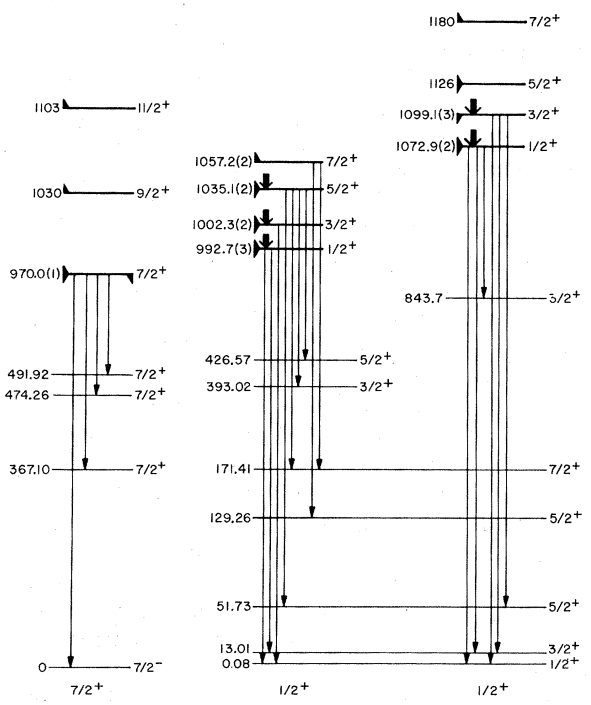

FIG. 9. States identified in the $\frac{7}{2}^+$ at 970.0-, $\frac{1}{2}^+$ at 922.7-, and $\frac{1}{2}^+$ at 1072.9-keV bands. For further details refer to the legend for Fig. 5.

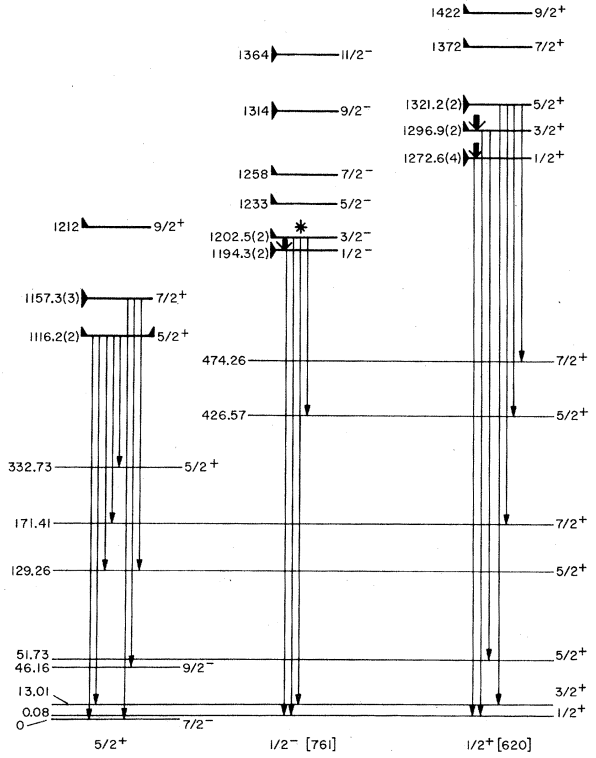

FIG. 10. States identified in the $\frac{5}{2}^+$ at 1116.2-keV, $\frac{1}{2}^-[761]$, and $\frac{1}{2}^+[620]$ bands. For further details refer to the legend for Fig. 5.

this case, both Rost and Nilsson calculations predict only modest strength in the $\frac{15}{2}^-$ member and this state would not be expected to be as predominant in the (^{3}He, α) results as other $\frac{15}{2}^-$ states.

T. $\frac{3}{2}^-$ Band at 1242.7 keV

The reaction ^{235}U$(d, d')^{235}$U populates the band head of a $\frac{3}{2}^-$ band (Fig. 11) at 1242.7 keV, which suggests some admixture of $(K-2)$ γ vibration on the $\frac{7}{2}^-$[743] band. The band has a fairly large amount of single-particle strength, and could contain part of the $\frac{3}{2}^-$[752] band, although the value of A^2 for the $\frac{7}{2}^-$ member is considerably smaller than the calculated value. The $\frac{15}{2}^-$ member of this band could be included in the strong 1737-keV excitation observed in the (^{3}He, α) reaction.[15]

U. $\frac{1}{2}^+$[620]

The measured spectroscopic strength of the $\frac{1}{2}^+$[620] band (Fig. 10) is about 70% of the predicted strength, suggesting that it is a fairly pure Nilsson state. The value of A^2 for the $\frac{7}{2}^+$ member is much smaller than predicted. The high-energy (n, γ) transition to the $\frac{1}{2}^+$ and $\frac{3}{2}^+$ states, and the suggested $l_n = 2$ angular momentum transfer are consistent with the assignment.

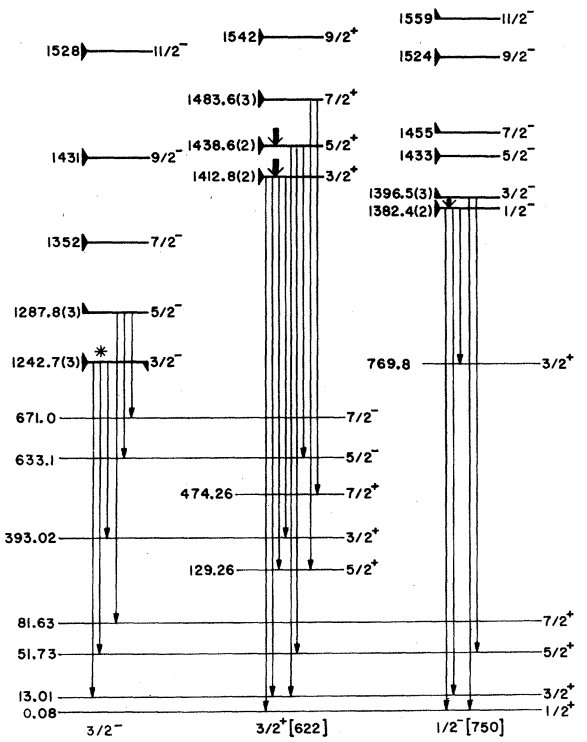

FIG. 11. States identified in the $\frac{3}{2}^-$ at 1242.7-keV, $\frac{3}{2}^+$[622], and $\frac{1}{2}^-$[750] bands. For further details refer to the legend for Fig. 5.

V. $\frac{1}{2}^-$[750]

About 75% of the predicted strength is observed to be contained in the $\frac{1}{2}^-$[750] band (Fig. 11), which suggests that it is a fairly pure single-particle state. The assignment is supported by the high-energy (n, γ) transition populating the $\frac{1}{2}^-$ state, and the suggested angular momentum transfer of $l_n = 1$ for the $\frac{3}{2}^-$ state. The $\frac{15}{2}^-$ member of this band may be included in the strong (^{3}He, α) excitation[15] at 1737 keV.

W. $\frac{3}{2}^+$[622]

From the measured spectroscopic strength one must conclude that the $\frac{3}{2}^+$[622] band (Fig. 11) contains a large particle-plus-phonon admixture. The $\frac{3}{2}^+$ level is excited by a primary transition in the (n, γ) reaction and a weak $E2$ transition feeds the $\frac{5}{2}^+$ level. Deexcitation proceeds to a variety of lower-lying levels with about three quarters of the intensity going to members of the $\frac{1}{2}^+$[631] and $\frac{3}{2}^+$[631] bands.

IV. INTERPRETATION OF RESULTS

The proposed level scheme based on the assignments of the previous section is summarized in Fig. 12. This level scheme contains 23 rotational bands, and 100 states up to 1600 keV in excitation energy. The actual level scheme of ^{235}U must, nevertheless, be far more complex than the one presented here. For example, there are 27 primary (n, γ) transitions observed to states (presumed to be mainly $J = \frac{1}{2}$ or $\frac{3}{2}$) below 1600 keV that are not included in the proposed level scheme. However, most of the observed single-particle strength [as measured in the (d, p) and (d, t) reaction] is included in the proposed scheme. Thus, an interpretation involving the distribution of single-particle strength is appropriate. Caution must be used in such an attempt, however, because of the high level density. In spite of the evidence supporting assignments made in the present work, some of these assignments are open to question. Therefore, an attempt will be made to present an interpretation of the level scheme which draws on simple considerations in order to explain the general features of the data.

Some insight into the distribution of single-particle strength can be gained by examining the Nilsson predictions.[17] Figure 13 shows the predicted excitation energies[17] of the Nilsson states in ^{235}U, corrected for pairing, plotted against the predicted values[21] of U^2. For comparison, Fig. 13 includes the known vibrational bands of ^{234}U.[5,6] Of first interest are two pairs of states connected by

dashed lines. Here are two cases of states with the same spin and parity, but quite different values of U^2 which would have similar excitation energies. Soloviev[20] has suggested that phonon mixing into single-particle states should cause these states to mix, producing states with anomalous values of U^2. The mixing of the $\frac{1}{2}^+$ states might be sizable, since they lie close to the energies of the core excitations. It is also clear from Fig. 13 that particle + phonon mixing may be extensive, since almost all spins and parities can be obtained in numerous ways by coupling a single-particle state to a phonon.

The excitation energies and values of U^2 for the band heads assigned in the present work are shown in Fig. 14. There are several bands with anomalous values of U^2, the most common being $\frac{1}{2}^+$ and $\frac{5}{2}^+$ bands. Furthermore, the greatest anomalies occur at excitation energies corresponding to those of the core excitations. Since this is the prediction of the particle + phonon mixing theory,[20] it seems reasonable that the anomalous values of U^2 can be used to identify the relative admixtures of specific single-particle states.

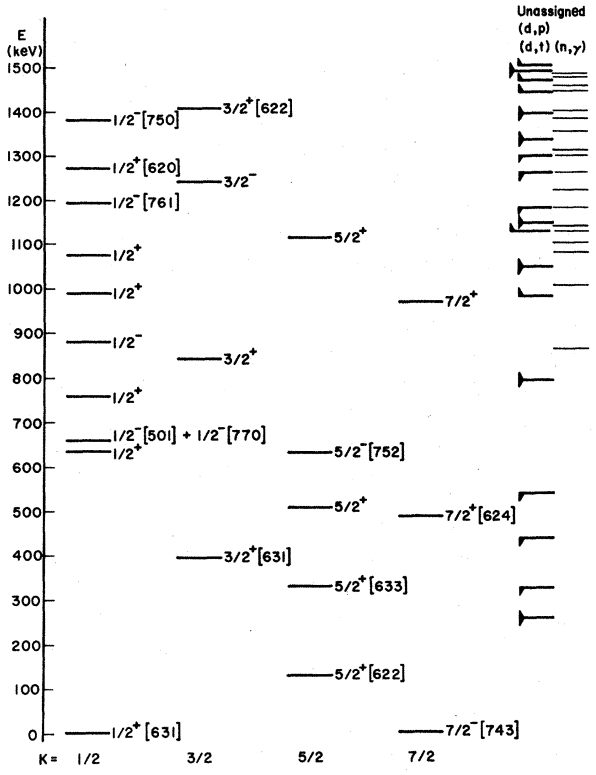

FIG. 12. Final level scheme for ^{235}U. Band heads of the various bands shown in Figs. 5–11 are shown and appropriate asymptotic quantum numbers are indicated. Individual unassigned levels from the (d,p), (d,t), and (n,γ) reactions are shown.

In a qualitative sense an anomalous value of U^2 has an obvious meaning. If only two Nilsson states of a given K^π are expected, one with $U^2 \cong 1$ and the other with $U^2 \cong 0$, then an observed state of the same K^π and $U^2 = 0.5$ should contain roughly equal admixtures of the two Nilsson states. More quantitatively, the value of U^2 for a mixed band might be written:

$$U^2 = \sum_i a_i u_i^2 / \sum_i a_i ,$$

where the a_i are the contributions from the individual Nilsson states, and the u_i^2 are the occupation probabilities for the unmixed Nilsson states. Thus, if only two Nilsson states are mixed, the amplitude of each component can be determined from the experimental value of U^2 and the experimental single-particle strength assuming theoretical values for u_i^2.

This method is used below to attempt to qualitatively determine the strength of various expected single-particle components in the observed bands for ^{235}U. In addition to the assumption that a mixed band has a U^2 equal to the weighted average of its single-particle components the analysis presented below relies heavily on the correct identification of the major single-particle states which contribute strength to a particular observed

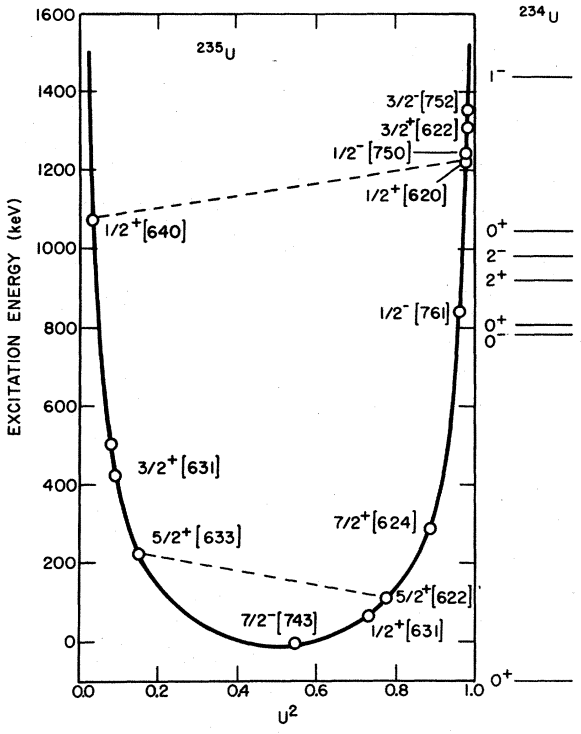

FIG. 13. Predicted band-head energies for Nilsson states in ^{235}U vs U^2. Band-head energies for known phonon states in ^{234}U are included at the right.

rotational band. The model assumes that if two single-particle states (1 and 2) contribute to a particular observed state, the relative contribution from each state (f_1 and f_2 where $f_1+f_2=1$) can be obtained from the experimental U^2 value and then the fraction of the strength from a particular single-particle state i is given by

$$a_i = f_i \times (\sum_j A_j^2),$$

where the A_j^2 are the measured spectroscopic amplitudes for the states in the observed band. For many of the observed bands the sum of the single-particle strength is considerably less than 1, indicating the presence of multi-quasiparticle components that are not excited in single-nucleon-transfer reactions. These multiquasiparticle components are assumed to arise primarily from admixtures of low-lying single-phonon excitations. The gross assumptions of the simple model described above are similar to a more detailed theoretical model recently presented by Gareev *et al.*,[20] and a comparison with their theoretical mixing calculations for ^{235}U is presented below where appropriate.

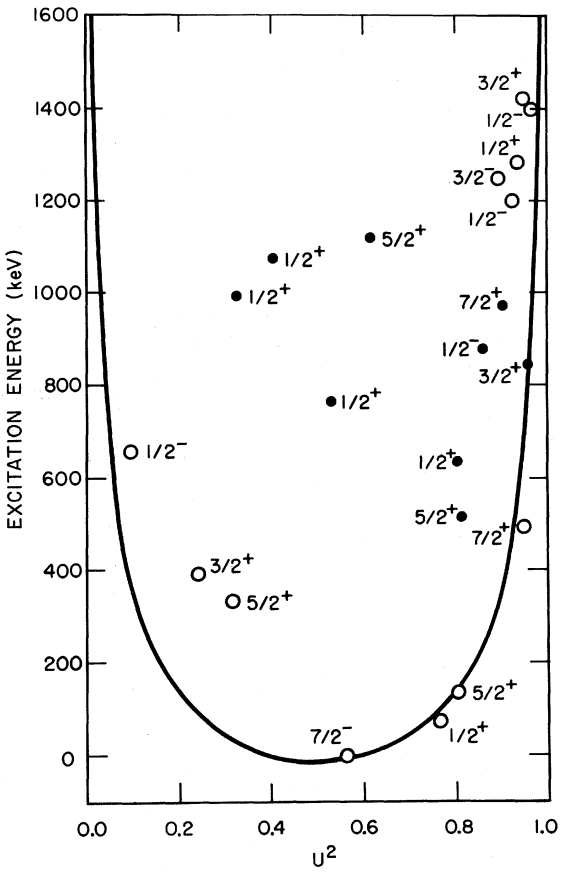

FIG. 14. Experimentally determined band-head energies vs experimental values of U^2. Spin assignments are indicated. The BCS calculation of U^2 is shown for comparison.

A. $K^\pi = \frac{1}{2}^+$ Bands

The single-particle strength of the $\frac{1}{2}^+$ band at 80 eV is probably due to the $\frac{1}{2}^+[631]$ Nilsson state exclusively. The measured single-particle strength is then 83% $\frac{1}{2}^+[631]$. The measured value $U^2=0.76$ is consistent with this conclusion. The $\frac{1}{2}^+$ band at 640.4 keV has a measured $U^2=0.81$, which, within experimental error, is the value expected for the $\frac{1}{2}^+[631]$ state. It is thus reasonable to assume that the 640.4-keV band is a second component of the $\frac{1}{2}^+[631]$ state, containing approximately 10% of the $\frac{1}{2}^+[631]$ strength. The $\frac{1}{2}^+[631]$ strength is almost completely exhausted by these two bands.

It is unlikely that the $\frac{1}{2}^+$ bands at 992.8 or 1072.7 keV contain significant $\frac{1}{2}^+[631]$ strength. Both of these bands have anomalous values of U^2: 0.33 and 0.41, respectively. It is reasonable to assume that the single-particle strength of both bands is a mixture of $\frac{1}{2}^+[640]$ strength and $\frac{1}{2}^+[620]$ strength. If the "unperturbed" values of U^2 for the $\frac{1}{2}^+[640]$ and $\frac{1}{2}^+[620]$ bands are assumed to be 0.04 and 0.98, respectively, (see Fig. 13), then the measured values of U^2 and the measured single-particle strengths can be obtained by assuming the 992.8-keV band to be 40% $\frac{1}{2}^+[640]$ plus 17% $\frac{1}{2}^+[620]$, and the 1072.7-keV band to be 20% $\frac{1}{2}^+[640]$ plus 11% $\frac{1}{2}^+[620]$. The $\frac{1}{2}^+$ band at 1272.6 keV has a measured U^2 of 0.93. The relative spectroscopic strengths of the members of the band indicate that the band is predominantly $\frac{1}{2}^+[620]$. The predicted value of U^2 for the $\frac{1}{2}^+[620]$ band is approximately 0.97, which agrees with the measured value to within experimental error. If the band-mixing concept is correct, however, a very small admixture of $\frac{1}{2}^+[640]$ strength might be expected. The results of the experiment can be reproduced by assuming the 1272.6-keV band to be 68% $\frac{1}{2}^+[620]$ plus 3% $\frac{1}{2}^+[640]$, although the $\frac{1}{2}^+[640]$ admixture is not strictly required. The weak $\frac{1}{2}^+$ band at 760.9 keV also has an anomalous value of $U^2=0.46$. This value could be obtained by mixing a small $\frac{1}{2}^+[640]$ strength with a small strength from either or both the $\frac{1}{2}^+[620]$ and the $\frac{1}{2}^+[631]$ bands. If the $\frac{1}{2}^+[620]$ component is assumed to be 4% then the experimental U^2 gives a mixture 8% $\frac{1}{2}^+[631]$, 15% $\frac{1}{2}^+[640]$, and 4% $\frac{1}{2}^+[620]$.

The scheme presented above for the single-particle mixtures in the $\frac{1}{2}^+$ bands accounts for a total of 101% of the $\frac{1}{2}^+[631]$, 100% of the $\frac{1}{2}^+[640]$, and 63% of the $\frac{1}{2}^+[620]$ bands, which appears very reasonable. The estimated 20% uncertainty in ex-

tracting absolute spectroscopic information from the data leads to a similar uncertainty in these mixing coefficients.

This scheme appears qualitatively consistent with the calculation of Gareev *et al.*,[20] who predict a relatively pure $\frac{1}{2}^+[631]$ band and two bands at 1030 and 1170 keV which contain mixtures of $\frac{1}{2}^+[640]$ and $\frac{1}{2}^+[620]$ strength.

In addition, the ^{233}U$(t,p)^{235}$U data indicate that the $\frac{1}{2}^+$ band at 640.4 keV contains some particle + phonon strength based on the $\frac{5}{2}^+[633]$ band. The phonon excitation involved must be a 2^+ phonon, and it is reasonable to assume that the 2^+ phonon is the γ vibration.

B. $K^\pi = \frac{3}{2}^+$ Bands

Three $K^\pi = \frac{3}{2}^+$ bands have been assigned in the present work. The $\frac{3}{2}^+$ band at 393.0 keV contains 34% of the $\frac{3}{2}^+[631]$ strength. The value of U^2 for this band is higher than the BCS prediction, but this discrepancy is not considered to be significant. The $K = \frac{3}{2}^+$ band at 843.7 keV is probably a positive-parity band. The relative spectroscopic factors indicate that it may be a component of the $\frac{3}{2}^+[622]$ band, containing 35% of the $\frac{3}{2}^+[622]$ strength. The $\frac{3}{2}^+$ band at 1412.8 keV also resembles the $\frac{3}{2}^+[622]$ state, and would contain 16% of its strength. The experimental values $U^2 = 0.95$ for both bands are identical. This value is consistent with the value of U^2 predicted for the $\frac{3}{2}^+[622]$ band. The calculations of Gareev *et al.*[20] predict a portion of the $\frac{3}{2}^+[622]$ band at 1290 keV.

C. $K^\pi = \frac{5}{2}^+$ Bands

The $\frac{5}{2}^+$ bands might be expected to contain admixtures of both the $\frac{5}{2}^+[622]$ and $\frac{5}{2}^+[633]$ Nilsson bands (see Fig. 13). The three lowest-lying bands do not seem to require such mixing. The $\frac{5}{2}^+$ band at 129.26 keV can simply be interpreted as 67% of the $\frac{5}{2}^+[622]$ band, and its U^2 of 0.80 is consistent with this. The single-particle strength of the $\frac{5}{2}^+$ band at 332.72 keV is probably 42% $\frac{5}{2}^+[633]$. The measured value of U^2 is 0.31, which is higher than would be expected from the BCS theory, but not significantly so. The $\frac{5}{2}^+$ band at 507.7 keV has a measured U^2 of 0.81, almost identical to that of the 129.26-keV band. The single-particle strength of the 507.7-keV band is therefore assumed to have predominantly (about 17%) $\frac{5}{2}^+[622]$ strength. The $\frac{5}{2}^+$ band at 1116.2 keV has a measured U^2 of 0.62. This is assumed to be a mixed $\frac{5}{2}^+$ band with the one quasiparticle strength being 14% $\frac{5}{2}^+[622]$ and 10% $\frac{5}{2}^+[633]$.

The reaction ^{233}U$(t,p)^{235}$U populates the band heads of the 507.7- and 1116.2-keV bands. Both of these must then contain some component in which the $\frac{5}{2}^+[633]$ state is coupled to a 0^+ phonon. For the 507.7-keV band, the 0^+ phonon is probably the β vibration. In the case of the 1116.2 keV state the nature of the phonon involved is not clear although it could, of course, be the β vibration. There is, however, a second 0^+ state in ^{234}U at 1044 keV. This state may be in part the pairing vibration, and may be the 0^+ phonon responsible for the 1116.2-keV band in ^{235}U.

D. $K^\pi = \frac{7}{2}^+$ Bands

Two $\frac{7}{2}^+$ bands have been assigned in the present work, and they both resemble components of the $\frac{7}{2}^+[624]$ Nilsson state. With this interpretation the 491.9-keV band contains 13% of the $\frac{7}{2}^+[624]$ strength, and the 970.0-keV band contains approximately 90% of the $\frac{7}{2}^+[624]$ strength. The $\frac{7}{2}^+[613]$ band, predicted to lie at about 1120 keV, has not been located in the present work. It should, however, have relative cross sections which are quite different from those of the 970.0-keV band.

The data from the reaction ^{235}U$(d,d')^{235}$U indicate that the 970.0-keV band also contains a component in which the 0^- octupole phonon is coupled to the $\frac{7}{2}^-[743]$ ground state.

E. $K^\pi = \frac{1}{2}^-$ Bands

Four $K^\pi = \frac{1}{2}^-$ bands have been assigned in the present work. The band at 659.0 keV has a predominantly hole character, with a U^2 of 0.09. The suggested interpretation of this band is that it is a mixture of the Nilsson $\frac{1}{2}^-[501]$ and $\frac{1}{2}^-[770]$ states, arising from the so-called "$\Delta N = 2$ mixing." On the basis of the Rost calculation for $\beta = 0.240$ the single-particle strength of the band is 90% ($\frac{1}{2}^-[501] + \frac{1}{2}^-[770]$). This must be considered an estimate, since there are many unknown factors in the "$\Delta N = 2$" mixing problems. The calculations of Gareev *et al.*[20] yield two states with mixtures of the $\frac{1}{2}^-[501]$ and $\frac{1}{2}^-[770]$ orbitals at energies of 430 and 760 keV.

The other three $K^\pi = \frac{1}{2}^-$ bands have a predominantly particle character. The one-quasiparticle strength of the bands is undoubtedly due to the $\frac{1}{2}^-[750]$ and $\frac{1}{2}^-[761]$ Nilsson states. The two bands at 1194.3 and 1382.4 keV are separated by only 188 keV, and could involve some mixing of the two Nilsson states. There is no clear evidence for this in the data. The relative spectroscopic strengths suggest that the 1194.3-keV band is 78% $\frac{1}{2}^-[761]$, and the 1382.4-keV band is 75% $\frac{1}{2}^-[750]$. The agreement with the Rost or Nilsson predictions is not very good; the suggested assignments are primarily based on the strong $\frac{7}{2}^-$ and $\frac{11}{2}^-$ states for the $\frac{1}{2}^-[761]$ band, and the strong $\frac{9}{2}^-$ state for the $\frac{1}{2}^-[750]$ band. The nature of the $\frac{1}{2}^-$

band at 878.7 keV is uncertain. If the band were predominantly $\frac{1}{2}^-[761]$, the spectroscopic strength of the $\frac{7}{2}^-$ state should be much greater than that observed. Thus, the band may be predominantly $\frac{1}{2}^-[750]$. Unfortunately, the $\frac{9}{2}^-$ member was not observed, so that a $\frac{1}{2}^-[750]$ assignment is also rather uncertain. Moreover, if the band does contain $\frac{1}{2}^-[750]$ strength, then two components of the $\frac{1}{2}^-[750]$ band would bracket a strong component of the $\frac{1}{2}^-[761]$ band. While this is certainly not impossible, one might expect band mixing to be significant in the circumstances. Since there is little evidence available for a discussion of mixing in this case, the 878.7-keV band must be considered unexplained.

F. $K^\pi = \frac{3}{2}^-$ Bands

The predominantly $K-2$ γ vibration built on the ground-state band at 637.8 keV proposed by Stephens *et al.*[14] is in agreement with the experimental results presented here. The $\frac{3}{2}^-$ band at 1242.7 keV is a reasonable candidate for the $\frac{3}{2}^-[752]$ band, containing 84% of the $\frac{3}{2}^-[752]$ single-particle strength. The band head is also populated in the reaction $^{235}U(d, d')^{235}U$. This implies that the band is in part the $(K-2)$ γ vibration based on the $\frac{7}{2}^-[743]$ ground-state band. There is no clear evidence for other $\frac{3}{2}^-$ bands in the present work, although it must be remembered that the parity of the $\frac{3}{2}^-$ band at 843.7 keV is uncertain. The $\frac{3}{2}^-[761]$ band is predicted to be a hole state in ^{235}U, but was not observed. The predicted spectroscopic strength for this band is concentrated in the $\frac{15}{2}^-$ member, and it would be difficult to find such a band in the (d,p) or (d, t) reactions.

G. $K^\pi = \frac{5}{2}^-$ and $\frac{7}{2}^-$ Bands

Evidence for the $\frac{5}{2}^-[752]$ band at 633.1 keV has

TABLE VI. Suggested character of rotational bands of ^{235}U. The estimated percent contributions from specific single-particle bands are determined as described in the text. The possible contributions from coupling of single-particle states to single-phonon β $[Q(2, 0)]$, γ $[Q(2, 2)]$, and octupole $[Q(3, 0)]$ vibrations are indicated.

Band-head energy (keV)	K^π	Suggested character
0.0	$\frac{7}{2}^-$	100% $\frac{7}{2}^-[743]$
0.08	$\frac{1}{2}^+$	82% $\frac{1}{2}^+[631]$
129.26	$\frac{5}{2}^+$	67% $\frac{5}{2}^+[622]$
332.7	$\frac{5}{2}^+$	42% $\frac{5}{2}^+[633]$
393.0	$\frac{3}{2}^+$	34% $\frac{3}{2}^+[631]$
491.9	$\frac{7}{2}^+$	13% $\frac{7}{2}^+[624]$
507.7	$\frac{5}{2}^+$	17% $\frac{5}{2}^+[622]$; $\frac{5}{2}^+[633] + Q(2, 0)$
633.1	$\frac{5}{2}^-$	$\frac{5}{2}^-[752]$
640.4	$\frac{1}{2}^+$	10% $\frac{1}{2}^+[631]$; $\frac{5}{2}^+[633] + Q(2, 2)$
659.0	$\frac{1}{2}^-$	90% $(\frac{1}{2}^-[501] + \frac{1}{2}^-[770])$
760.9	$\frac{1}{2}^+$	12% $\frac{1}{2}^+[641]$; 15% $\frac{1}{2}^+[640]$; 6% $\frac{1}{2}^+[620]$
843.7	$\frac{3}{2}^+$	35% $\frac{3}{2}^+[622]$
878.7	$\frac{1}{2}^-$	? $\frac{1}{2}^-[750]$; ? $\frac{1}{2}^-[761]$
970.0	$\frac{7}{2}^+$	90% $\frac{7}{2}^+[624]$; $\frac{7}{2}^-[743] + Q(3, 0)$
992.8	$\frac{1}{2}^+$	40% $\frac{1}{2}^+[640]$; 17% $\frac{1}{2}^+[620]$
1072.7	$\frac{1}{2}^+$	20% $\frac{1}{2}^+[640]$; 11% $\frac{1}{2}^+[620]$
1116.2	$\frac{5}{2}^+$	14% $\frac{5}{2}^+[622]$; 10% $\frac{5}{2}^+[633]$; $\frac{5}{2}^+[633] + K = 0$ phonon
1194.3	$\frac{1}{2}^-$	78% $\frac{1}{2}^-[761]$
1242.3	$\frac{3}{2}^-$	84% $\frac{3}{2}^-[752]$; $\frac{7}{2}^-[743] + Q(2, 0)$
1273	$\frac{1}{2}^+$	68% $\frac{1}{2}^+[620]$; 3% $\frac{1}{2}^+[640]$
1382.5	$\frac{1}{2}^-$	75% $\frac{1}{2}^-[750]$
1412.8	$\frac{3}{2}^+$	16% $\frac{3}{2}^+[622]$

been found in the ^{234}U$(n,\gamma)^{235}$U data. This assignment agrees with that of Stephens.[14] The band is not populated in the (d,p) or (d,t) reactions, which is consistent with the extremely small spectroscopic strengths predicted for the low-spin members. Thus, no information is available as to the strength of the single-particle character of the band.

The $\frac{7}{2}^-[743]$ band is the ground-state band of ^{235}U, and was observed to be an essentially pure single-particle band.

V. SUMMARY

A summary of the considerations in the previous section is given in Table VI. It should be stressed that this is only a semiquantitative interpretation of the experimental results. It does, however, present a coherent picture of the distribution of single-particle strength. If one accepts the general basis of this interpretation as being reasonable, the results can be compared with the Nilsson model's prediction of band-head energies.[17] In order to do this, a "center of gravity" must be estimated for the components of each Nilsson state. If all components were located, then such an estimate could be obtained from:

$$\bar{E}_j = \sum_i a_{ij} E_i / \sum_i a_i ,$$

where a_{ij} is the strength of a particular single-particle state, j, in the experimentally observed band, i, with band-head energy E_i. Even though in some cases in the present work not all components have been observed, a qualitative estimate may still indicate trends. Figure 15 shows a comparison of Nilsson predictions of experimental single-particle strength, with estimates of the "centers of gravity" included where applicable. It is interesting to see that the estimated experimental center of gravity of $\frac{1}{2}^+[631]$ strength lies at 124 keV, in rough agreement with Nilsson's prediction, even though the major component of $\frac{1}{2}^+[631]$ strength is essentially degenerate with the ground state.

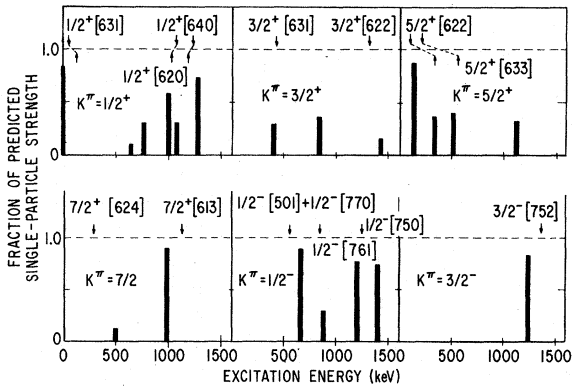

FIG. 15. Suggested distribution of single-particle strength in ^{235}U summed over each rotational band. The theoretical limit of 1 is shown. Predicted band-head energies are shown above the dashed lines, extracted "center of gravity" below the dashed lines.

The level structure of ^{235}U is clearly affected by vibrational admixtures. These admixtures fragment the states predicted by the Nilsson model. It seems, however, that a reasonable picture of the distribution of single-particle strength can be obtained. The anomalous values of U^2 observed are a great aid in this interpretation, and a more accurate treatment of these anomalies might be a valuable tool for future work. The use of several reactions in this investigation has proved essential, since for extensive analysis there are many uncertainties involved in the data obtained from any one reaction. A comprehensive view of the level structure seems to be necessary in order to realistically approach the problem of band mixing in actinide nuclei.

ACKNOWLEDGMENT

The authors are indebted to the Los Alamos scanning group for the many hours spent scanning photographic plates, and to Mrs. Judith Gursky and J. G. Povelites for preparation of the targets used in this experiment. We gratefully acknowledge helpful discussions with M. E. Bunker, B. Mottelson, E. Rost, and R. Sheline.

APPENDIX

DWBA Calculations for the Direct-Reaction Calculations and Their Use

The purpose of this Appendix is to discuss the DWBA calculations and the reliability of the spectroscopic information obtained.

The DWBA code JULIE[9] was used in the calculations, with spin-orbit strengths set to zero throughout. The standard prescription for calculating reaction amplitudes for reactions involving spherical nuclei is to represent the relative wave functions for the initial and final systems by elastic scattering wave functions. In the case of a deformed nucleus this approximation is not as good, since the first excited state is usually a rotational state at a low excitation energy which is strongly coupled to the ground state. These inelastic excitations should be included in a description of the initial and final systems, and might be described by coupled-channel wave functions. The code JULIE will only calculate optical-

model wave functions, and they must be adjusted in some way to approximate the more realistic coupled-channel calculation. These considerations are discussed in detail by Elbek and Tjøm.[1] In the present work this was crudely done by fitting the combined cross sections for the ground and first excited states with the optical model. Angular distributions for the scattering of 20-MeV protons, deuterons, and tritons to the 0^+ and 2^+ states of ^{234}U were measured using the optical-model code of Perey.[22] The data and best-fit theoretical curves are shown in Fig. 16. The parameters of the fits are given in Table VII. The Woods-Saxon well for the bound-state calculation was described by the Rost parameters for ^{209}Pb,[18] with the well depth adjusted to give the correct binding energy. The fixed parameters were $r_0 = 1.349$ F and $a = 0.70$ F.

The JULIE calculations for the reaction ^{234}U(d,p)-^{235}U yielded angular distributions for different l transfers which were easily distinguishable as can be seen in Fig. 2. These calculations were used to extract l transfers for some of the states observed experimentally. Determining l values was made difficult by the high density of states. A least-squares-fitting code was used to resolve close doublets, but the areas obtained were not as accurate as the energies. There were also many states for which the number of counts was too low to allow l-value assignments.

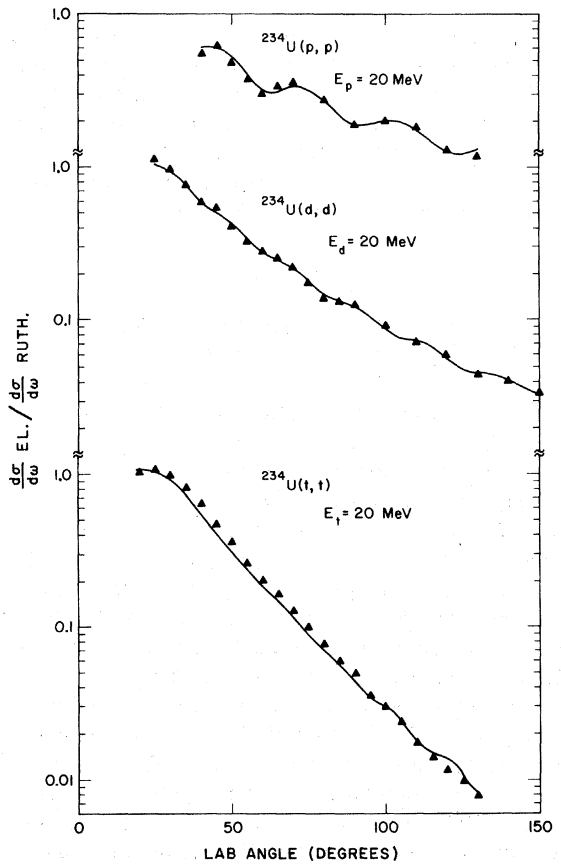

FIG. 16. Optical-model fits to elastic scattering measurements.

TABLE VII. Optical-model parameters.

Particle	V_s (MeV)	r_{0s} (F)	a_s (F)	W_d (MeV)	W_s (MeV)	r_{0I} (F)	a_I (F)
Proton	43.3	1.347	0.603	18.5	0	1.20	0.695
Deuteron	71.9	1.347	0.729	24.9	0	1.34	0.663
Triton	168.3	1.24	0.684	0	14.52	1.45	0.987

Calculations for the reaction ^{236}U$(d, t)^{235}$U did not yield sufficiently distinctive angular distributions for l-value determinations. The calculations gave good fits to the data where l transfers were known, however, and were used in order to extract spectroscopic information.

The accuracy of the spectroscopic quantities (A^2, U^2, V^2) depends on the accuracy of the DWBA calculations. Although there is some uncertainty as to the absolute normalization of the calculation, relative magnitudes for various l values should be quite good. Errors in the absolute magnitudes of the (d,p) and (d, t) calculations would thus be expected to produce a constant normalization error for all of the spectroscopic strengths measured in the present work. The most reasonable estimate of this error comes from a comparison with nuclear-structure theory.

Nuclear-structure theory states that for a pure Nilsson state the sum of spectroscopic strengths over all members of a band must equal 1. Particle + phonon mixing calculations show that the strength of a Nilsson state is fragmented, giving rise to a general dilution of single-particle strength in individual rotational bands. These same calculations, however, indicate that the ground-state rotational band usually rises from a rather pure Nilsson band. The ground-state band of ^{235}U is the $\frac{7}{2}^-[743]$ band, where unfortunately several members are obscured. For the members observed, the sum of experimental spectroscopic strengths can be compared with theory, and is seen in Table V to be 13% higher than the Nilsson prediction, which is within the estimated experimental error. Moreover the values of $U^2 = 0.56$ and $V^2 = 0.44$ extracted from the data are consistent with the values expected for the ground state. Thus, in the present results there is no experimental evidence of errors in the absolute magnitudes of the JULIE reaction amplitude calculations.

*Work performed under the auspices of the U. S. Atomic Energy Commission.

[1]B. Elbek and P. O. Tjøm, in *Advances in Nuclear Physics*, edited by M. Baranger and E. Vogt (Plenum, New York, 1969), Vol. 3, p. 259.
[2]S. G. Nilsson, Kgl. Danske Videnskab. Selskab, Mat.-Fys. Medd. 29, No. 16 (1955).
[3]D. G. Burke, B. Zeidman, B. Elbek, B. Herskind, and M. C. Olesen, Kgl. Danske Videnskab. Selskab, Mat.-Fys. Medd. 35, No. 2 (1966).
[4]F. A. Rickey, Jr., and R. K. Sheline, Phys. Rev. 170, 1157 (1968).
[5]L. A. Malov, V. G. Soloviev, and P. Vogel, Phys. Letters 22, 441 (1966).
[6]S. Bjørnholm, M. Lederer, F. Asaro, and I. Perlman, Phys. Rev. 130, 2000 (1963).
[7]T. H. Braid, R. R. Chasman, J. R. Erskine, and A. M. Friedman, Phys. Rev. C 1, 275 (1970).
[8]J. Borggren, B. Elbek, and L. P. Nielsen, Nucl. Instr. Methods 24, 1 (1963).
[9]R. M. Drisko, unpublished.
[10]E. T. Jurney, H. T. Motz, and S. H. Vegors, Jr., Nucl. Phys. A94, 351 (1967).
[11]*Neutron Cross Sections*, compiled by J. R. Stehn, M. D. Goldberg, R. Wiener-Chasman, S. F. Mughabghab, B. A. Magurno, and V. M. May, Brookhaven National Laboratory Report No. BNL-325(U. S. GPO, Washington, D. C., 1966), 2nd ed., 2nd Suppl., Vol. II, $Z=88$ to 98.
[12]A. Bohr and B. R. Mottelson, Kgl. Danske Videnskab. Selskab, Mat.-Fys. Medd. 27, No. 16 (1953).
[13]C. M. Lederer, J. M. Hollander, and I. Perlman, *Table of Isotopes* (Wiley, New York, 1968), 6th ed.
[14]F. S. Stephens, M. D. Holtz, R. M. Diamond, and J. O. Newton, Nucl. Phys. A115, 129 (1968).
[15]Th. W. Elze and J. R. Huizenga, Nucl. Phys. A133, 10 (1969).
[16]E. Rost, Phys. Rev. 154, 994 (1967).
[17]R. K. Sheline, W. N. Shelton, T. Udagawa, E. T. Jurney, and H. T. Motz, Phys. Rev. 151, 1011 (1966).
[18]E. Rost, Phys. Letters 26B, 184 (1968).
[19]M. E. Bunker, private communication.
[20]V. G. Soloviev, in Proceedings of the International Symposium on Nuclear Structure, Dubna, 1968 (unpublished); F. A. Gareev, S. P. Ivanova, L. A. Malov, and V. G. Soloviev, Nucl. Phys. A171, 134 (1971).
[21]S. T. Belyaev, Kgl. Danske Videnskab. Selskab, Mat.-Fys. Medd. 31, No. 11 (1959).
[22]C. M. Perey and F. G. Perey, Phys. Rev. 132, 755 (1963).

PHYSICAL REVIEW C VOLUME 5, NUMBER 6 JUNE 1972

Gamma-Ray Studies of the Decays of ^{92}Kr, ^{92}Rb, and ^{92}Sr

R. J. Olson, W. L. Talbert, Jr., and J. R. McConnell
Ames Laboratory, U. S. Atomic Energy Commission and Department of Physics, Iowa State University, Ames, Iowa 50010
(Received 17 February 1972)

Measurements made with Ge(Li) detectors are reported for γ-ray transition energies and intensities observed following the β decay of the neutron-rich nuclei ^{92}Kr, ^{92}Rb, and ^{92}Sr. These nuclides are members of the isobaric decay chain for $A=92$ beginning with ^{92}Kr, which was obtained using the on-line isotope-separator system TRISTAN developed for the study of gaseous fission-product activities. Level schemes have been constructed for ^{92}Rb, ^{92}Sr, and ^{92}Y with the aid of Ge(Li)-Ge(Li) coincidence results. Some of the energy levels found are considered from a shell-model approach.

I. INTRODUCTION

This work is one of a series of studies[1-5] made on neutron-rich gaseous fission products of ^{235}U with the TRISTAN on-line isotope-separator system.[6] The results reported here are based on measurements of γ transitions following the β decay of ^{92}Kr, ^{92}Rb, and ^{92}Sr. The γ-ray transition energies, relative intensities, and observed γ-γ coincidences are reported, along with the level schemes constructed from this information. The deduced logft values are used in conjunction with relative photon transition probabilities as a partial basis for tentative level spin and parity assignments. In many cases, these assignments are suggestive of quasiparticle configurations appropriate in this mass region from shell-model considerations.

The general purpose behind a project such as this is to fill in gaps in the comparison of nuclear properties across the nuclidic chart. Systematic trends established previously have led to developments of nuclear models and the division of nuclei into three groups on the basis of spherical, deformed, or intermediate characteristics. It is expected that the systematic collection of more evidence for the properties of nuclei far from the line of β stability will lead to a deeper understanding of the properties of the nuclear force. The investigation of level schemes following the β decay of